Electronic properties of carbon nanotubes

J. González
Instituto de Estructura de la Materia
Consejo Superior de Investigaciones Científicas
Serrano 123, 28006 Madrid. Spain.

November 28, 2002

Contents

Review chapter contributed to the
Encyclopedia of Nanoscience and Nanotechnology
(American Scientific Publishers, 2003)

1 Introduction

Carbon nanotubes are tubular structures that can be thought of as the result of wrapping up the carbon honeycomb lattice of a graphene sheet. They were discovered in 1991 with the use of high-resolution transmission-electron microscopy, by observing the soot produced from an arc discharge between carbon rods[1]. Since then they have been a fascinating subject of research due to their remarkable mechanical, chemical and electronic properties[2]. Carbon nanotubes have become very promising in the field of molecular electronics, in which atoms and molecules are envisaged as the building blocks in the fabrication of electronic devices. In this respect, the great expectatives placed on the nanotubes are also shared by the fullerenes[3]. These also can be thought as being assembled from the hexagonal carbon rings of a graphene sheet, by making a close cage by insertion of twelve pentagonal rings. The multiple forms and shapes in which the carbon-based materials may appear, with varying physical and chemical properties, is what makes them so interesting for the purpose of designing and fabricating nanoscale devices.

The nanotubes as well as the fullerenes have a molecular structure that makes them particularly suitable to develop an alternative, at the nanometer scale, to the silicon-based integrated electronics. It is known, for instance, that nanotubes have a remarkable stifness along the tubular direction, reinforcing the structure of the components based on them. On the other hand, the design of electronic devices at the molecular scale requires taking into account novel effects which stem from the reduced dimensionality of the systems under consideration. In the case of individual single-walled nanotubes at low temperatures, it has been shown that the electron waves may remain extended along the nanotubes over lengths of several microns[4, 5]. This means that the motion of the electrons cannot be understood in terms of classical diffussion, and that instead they show a genuine quantum mechanical behavior, up to the point that interference patterns between the electron waves can be observed[6].

The behavior of the nanotubes as true quantum wires leads to remarkable predictions, like the ballistic transport along the longitudinal direction. This effect seems to have been observed in multi-walled nanotubes[7], which have an onion-like structure of concentric single-walled nanotubes. The very large current densities observed there (above 10^7 A cm^{-2}) seem to be only compatible with transport without dissipation in the nanotube structure. On the other hand, single-walled nanotubes are also commonly found forming close-packed ropes. Their behavior may give rise to interesting features, because the strong Coulomb repulsion between electrons existing in the isolated nanotubes is screened due to the intertube interactions between a large number of metallic nanotubes. A superconducting transition at temperatures below 1 K has been observed in ropes made of about three hundred nanotubes[8]. Superconductivity seems to be also a plausible phenomenon in small-diameter nanotubes, where the coupling of the electrons to lattice vibrations is largely enhanced[9].

The main goal in designing nanotechnology devices is to tailor the molecular structures to achieve a given functionality. In that respect, the various geometries that the nanotubes may adopt and the possibility of assembling them with

other carbon structures open the way to the construction of common electronic devices like diodes[10], transistors[11, 12, 13, 14], memory elements[15] and logic circuits[16, 17]. As explained below, the nanotubes may have metallic or semiconducting properties depending on the way the graphene sheet is wrapped[18, 19, 20]. The nanotube structure can change along the tubule from one class to the other by the presence of topological defects, that is, heptagonal and pentagonal rings in the hexagonal carbon lattice[21, 22, 23]. This kind of intramolecular junctions have shown diode-like rectifying properties[10]. Furthermore, transistors working with a single nanotube element have been produced, either by the field-effect on semiconducting nanotubes[11, 12, 13] or by constraining single electrons to short islands between two buckles in a metallic nanotube[14]. An alternative to these structures can be the use of Y-junctions in which two single-walled nanotubes merge into one at a given angle[24, 25]. The response characteristics of such devices have shown interesting properties, including nonlinear transport behavior and current rectification[26, 27, 28, 29].

One of the challenges of the carbon nanotube based molecular electronics is the controlled high-yield production of the relevant structures in the design of the electronic devices. The progress in the development of new techniques and the synthesis of new structures is constant. Very promising is the formation of supramolecular assemblies in which fullerene cages are inserted in the hollow structure of the nanotube[30, 31, 32]. It has been shown that the presence of the fullerenes leads to a modulation of the gap in the case of the semiconducing nanotubes[33]. When the fullerenes are disposed forming an array inside the nanotube, the hybridization of the fullerene molecular orbitals with the states in the nanotube conduction band gives rise to a band with mixed fullerene-nanotube character[34]. Surely the interplay between the properties of the carbon nanotubes and the electronic features of the fullerenes has to give rise to new physical effects, opening the way to different routes in the design of components in molecular electronics.

2 Metallic versus semiconducting nanotubes

2.1 Band structure of carbon nanotubes

A remarkable feature of the single-walled carbon nanotubes is that their conduction properties depend on the helical arrangement of the hexagonal carbon rings on the tubular structure. Thus, carbon nanotubes can be metallic or semiconducting as a consequence of their particular geometry and, when a gap develops in the low-energy spectrum, it also depends on the diameter of the nanotube. These properties follow from the band structure of the tubular arrangements, which is composed of a certain number of one-dimensional subbands depending on the thickness of the nanotube. The conducting properties can be formally ascertained by addressing the question of whether the Fermi level crosses or not some of the subbands. The prediction of the metallic and semiconducting properties of the nanotubes depending on their geometry was actually made on theoretical grounds in 1992 [18, 19, 20]. Although the electronic properties of the nanotubes had been studied for some time, it was not

until 1998 that their structrure was atomically resolved by using scanning tunneling microscopy[35, 36]. In this way, it has been possible to establish experimentally the correspondence between the conducting properties and the geometric structure of the individual single-walled nanotubes.

Except in cases where the nanotube diameter is very small[37, 38, 39], the band structure of the individual nanotubes can be understood from the band dispersion of a graphene sheet, after applying the periodic boundary conditions arising from the winding of the hexagonal rings around the axis of the nanotube. The conduction properties can be obtained qualitatively from the hybridization of the carbon π orbitals, which gives rise to respective bonding and antibonding bands in the graphite sheet. The two-dimensional Brillouin zone is an hexagon and the electron energy-momentum dispersion $E(\mathbf{k})$ takes the following form in the tight-binding approximation[40]:

$$E(\mathbf{k}) = \pm t\sqrt{1 + 4\cos^2(\sqrt{3}k_x a/2) + 4\cos(\sqrt{3}k_x a/2)\ \cos(3k_y a/2)} \qquad (1)$$

where a is the nearest-neighbor carbon-carbon distance (≈ 0.14 nm) and t is the energy scale (≈ 2.5 eV) given by the matrix element between neighboring π orbitals. The bonding π band of the dispersion relation (corresponding to the $-$ sign in front of the right-hand-side of Eq. (1)), has the shape depicted in Fig. 1. The cusps are attained at the corners of the hexagonal Brillouin zone, which correspond to the momenta

$$k_x = \pm\frac{4}{3\sqrt{3}}\frac{\pi}{a} \quad , \quad k_y = 0 \qquad (2)$$

$$k_x = \pm\frac{2}{3\sqrt{3}}\frac{\pi}{a} \quad , \quad k_y = \pm\frac{2}{3}\frac{\pi}{a} \qquad (3)$$

It has been shown that, for typical nanotubes with diameter above 1 nm, the carbon σ orbitals have a weak influence on the bonding π band, and that the bonding σ bands appear in the spectrum at energies below ~ -2 eV [18].

When the graphene sheet is not doped by impurities or other means, each carbon atom contributes with one electron to the above band structure which, taking into account the spin degeneracy, turns out to be half-filled. The Fermi level is found then at the cusps connecting the lower and upper branches of the band dispersion given by Eq. (1), so that the graphene sheet is a remarkable two-dimensional system which has a set of isolated Fermi points (only two of them being inequivalent) when the carbon lattice is half-filled.

The passage from the electronic states in the graphene sheet to those allowed in the carbon nanotubes can be made by enforcing the conditions satisfied by the electron wavefunctions when winding around the waist of the tubule. This is the point where the geometry of the nanotube plays a crucial role, since many different possibilities exist characterized by the helicity of the carbon lattice on the tubular structure. A simple instance is given by the so-called *zig-zag* nanotubes, in which the graphene lattice is wrapped in the direction depicted in Fig. 2, and that receive their name from the /\/\/\/\ shape perpendicular to the tube axis. Another significant

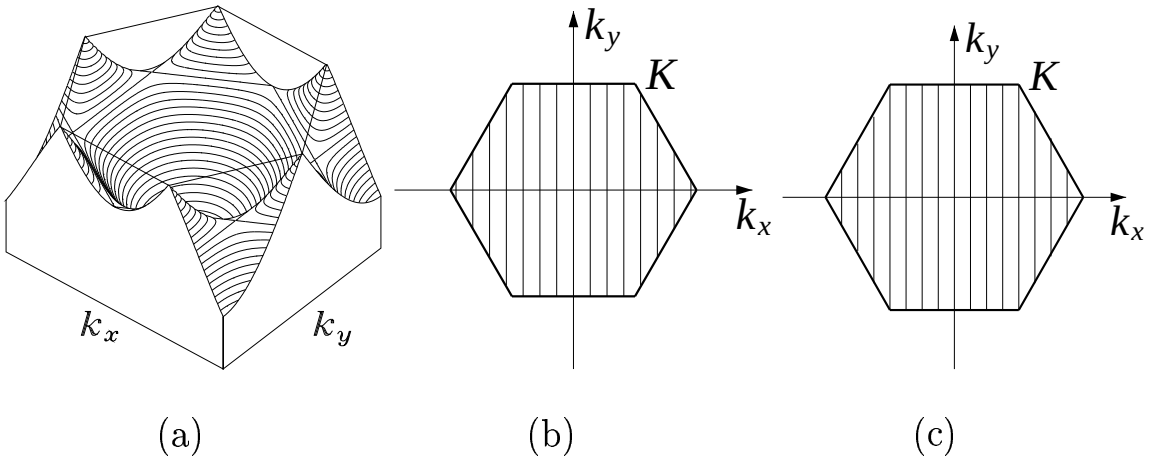

Figure 1: Representation of the first Brillouin Zone and band structure of graphene and carbon nanotubes. (a) Dispersion of the bonding π band in graphene. (b) Plot of the allowed wavevectors (vertical lines) in the first Brillouin Zone for a zig-zag nanotube with $N = 11$. (c) Same plot as in (b) for a zig-zag nanotube with $N = 12$.

case correspond to the *armchair* nanotubes, so-called because of the pattern /‾\ _/‾_/‾\ that they display after forming the tubular arrangement with the axis as depicted in Fig. 3.

The analysis of the zig-zag and the armchair nanotubes gives insight about the general argument by which a single-walled nanotube can be catalogued as metallic or semiconducting. The different subbands of a nanotube can be obtained from the band dispersion in Eq. (1) by taking into account that the electron wavefunction $\Psi(\mathbf{r})$ has to be single-valued after taking a close path around the tubule. Their dependence on the position $\mathbf{r}$ (measured with the coordinates of the graphene sheet) is of the form

$$\Psi(\mathbf{r}) \sim \exp(i\mathbf{k} \cdot \mathbf{r}) \tag{4}$$

This means that the argument of the exponential has to increase by a multiple of 2π times i after going once around the waist of the nanotube.

In the case of a zig-zag nanotube with lattice vector $\mathbf{T}_1$ in the direction perpendicular to the axis, as shown in Fig. 2, we must have

$$N\,\mathbf{T}_1 \cdot \mathbf{k} = 2\pi n \tag{5}$$

where N is the number of hexagons found when going around the nanotube and n is an integer number. The above constraint traslates into the quantization condition

$$k_x = \frac{2\pi}{\sqrt{3}a}\frac{n}{N} \tag{6}$$

which gives the allowed wavevectors in a zig-zag nanotube. These correspond to a certain number of straight lines in the Brillouin zone, that have been shown for the particular cases of $N = 11$ and $N = 12$ in Fig. 1. Each line corresponds to a

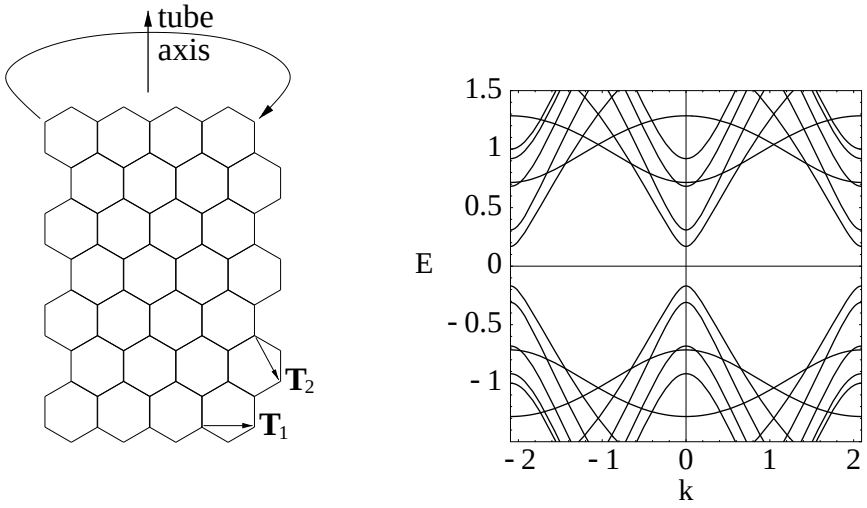

Figure 2: Left: Schematic representation of the wrapping action leading to a zig-zag nanotube. Right: Band structure of a zig-zag nanotube with $N = 11$ (the energy is measured in units of the overlap integral and the momentum in units of the inverse lattice spacing).

one-dimensional subband for the tubular structure. In general, an undoped carbon nanotube can have metallic properties only when there is some subband passing by the points where the bonding and antibonding bands meet. According to the Eqs. (2) and (3) and the quantization condition (6), that only happens in the case of a zig-zag nanotube when the number N of hexagons around the circumference is a multiple of 3 [18, 19]. A narrow gap may open, however, due to the different strength of the electron transfer in the direction perpendicular to the tube axis, which leads to a shift of the Fermi points (in the k_x direction) from the corners of the Brillouin zone. If the number N is not multiple of 3, a moderate gap Δ opens in the spectrum[18, 19], with a dependence on the diameter d of the form[2, 3]

$$\Delta = 2ta/d \tag{7}$$

This sensitive dependence of the conducting properties of the nanotubes is illustrated by the band structure of the zig-zag nanotube with $N = 11$ shown in Fig. 2.

Moving now to the case of the armchair nanotubes, the periodic boundary conditions imply a similar quantization condition on the component k_y of the momentum, which is now in the direction transverse to the tubule axis. Calling M the number of lattice periods along the circumference of the nanotube, the requirement of having single-valued wavefunctions leads to the condition

$$k_y = \frac{2\pi}{3a}\frac{n}{M} \tag{8}$$

n being again an integer number. The set of allowed wavevectors corresponds to a certain number of straight lines in the Brillouin zone, perpendicular to those found

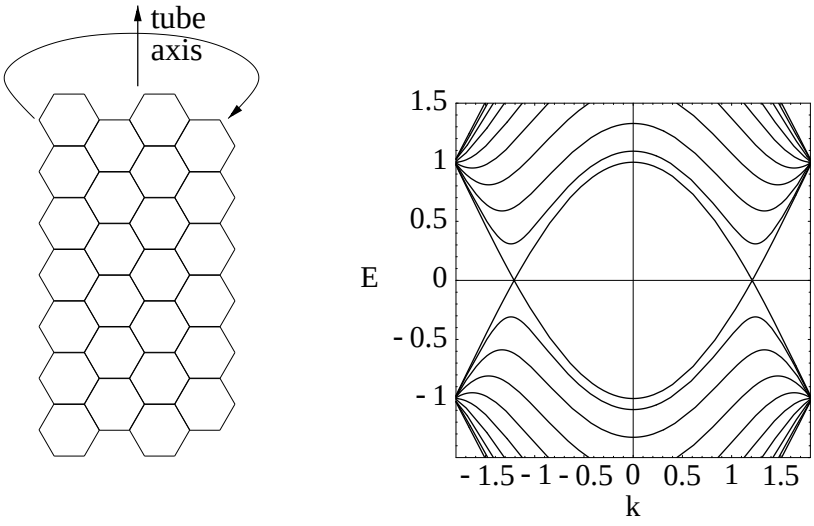

Figure 3: Left: Schematic representation of the wrapping that leads to an armchair nanotube. Right: Band structure of an armchair nanotube with $M = 10$ (in the same units as in Fig. 2).

in the case of zig-zag nanotubes. Now there is always a subband at the point where the bonding and antibonding π bands meet, irrespective of the value that M may take. This is shown in the band structure for $M = 10$ represented in Fig. 3. It turns out therefore that all the armchair nanotubes have subbands crossing the Fermi level, and that they remain metallic even taking into account the effects due to the curvature of the tubule[18, 19, 20].

The geometric structures of the zig-zag and the armchair nanotubes are special cases among all the possibilities by which the graphene sheet can be wrapped to form the nanotubes. The arrangement of the hexagonal carbon rings may show in general some helicity along the tubule. The construction of an helical arrangement can be visualized by starting from the lattice as depicted in Fig. 2, and rolling up the tubule, not in the direction of the hexagon rows, but wrapping a row of hexagons onto the next above or below when completing the turn around the tubule. Obviously, that operation can be also done by joining a row of hexagons with the second row, the third, etc. above or below the starting hexagon.

The helicity can be measured then by the shift of a number m of lattice vectors $\mathbf{T}_2$ (defined in Fig. 2) when wrapping the graphene sheet. The degree of helicity m and the number n of hexagons in the row of the parent zig-zag tubule characterize completely the geometric structure of the nanotube. These numbers are given usually in the notation (n, m). Thus, the zig-zag nanotubes are represented by the $(n, 0)$ geometric structures, while it can be checked that the (n, n) tubules correspond to the armchair nanotubes. Carbon nanotubes which do not have zig-zag or armchair structure are called *chiral* nanotubes. In the experiments, the (n, m) structure of the nanotube can be obtained from the measurements of the diameter of the tubule and the chiral angle ϕ formed by the tube axis and the rows of aligned hexagons.

The arguments allowing to understand the conduction properties of the zig-zag and the armchair nanotubes can be applied also to the general case of the chiral nanotubes. It turns out that these have subbands crossing the K point of the Brillouin zone when the geometric structure given by (n, m) is such that $n - m$ is a multiple of 3 [18, 19]. In that case, a narrow gap may open at the Fermi level due to the same curvature effects invoked for the zig-zag nanotubes. For the rest of chiral nanotubes, a moderate gap opens up in the spectrum, with a dependence on the nanotube diameter that follows the same law predicted for the zig-zag nanotubes.

2.2 Experimental measurements

The predictions regarding the sensitivity of the conducting properties on the geometric structure of the carbon nanotubes have been confronted in the experiments reported in Refs. [35] and [36]. In both experiments, individual single-walled nanotubes have been produced with the technique of laser vaporization, being deposited afterwards on a Au(111) substrate. In Ref. [36], measurements have been also reported on single-walled nanotubes at the surface of a rope. Topographic images of the individual nanotubes have been obtained at constant tunnel current in a scanning tunneling microscope, leading to the resolution of the hexagonal structure of the carbon rings. This has made possible to determine the degree of helicity which, together with the knowledge of the nanotube diameter, allows to identify the nanotube in the above catalogue given in terms of the (n, m) numbers.

Within the same experimental setting, scanning tunneling spectroscopy has been performed, in which the current I through the vacuum barrier between the STM tip and the nanotube is recorded as a function of the bias voltage V applied to the sample. This provides important information about the electronic structure, since the differential conductance dI/dV is proportional to the density of states in the nanotube. More precisely, the normalized differential conductance $(V/I)(dI/dV)$ seems to provide a good representation of the local density of electronic states[41]. From the measurements carried out in Refs. [35] and [36], it has been possible to determine the position of the peaks corresponding to the edges of the one-dimensional conduction and valence bands and the consequent gap in the semiconduting nanotubes.

Fig. 4 contains one of the atomically resolved images of single-walled nanotubes reported in the experiment of Ref. [36]. As discussed there, the dark dots correspond to hexagonal carbon rings, and the degree of helical arrangement can be easily discerned in the images. The angle formed between the rows of hexagons and the tube axis determines the chiral angle. The measured values of the angle and the diameter are consistent with the structure of a $(14, -3)$ nanotube, which should be a moderate gap semiconductor. The spectroscopy measurements show indeed a very small current for bias voltages between -300 and 400 mV. The peaks of the normalized differential conductance out of that range correspond to the edges of the one-dimensional subbands. As reported in Ref. [36], a gap can be estimated for the mentioned nanotube of the order of ≈ 750 meV. In general, in the measurements carried out in the semiconducting nanotubes the current seems to be very small but

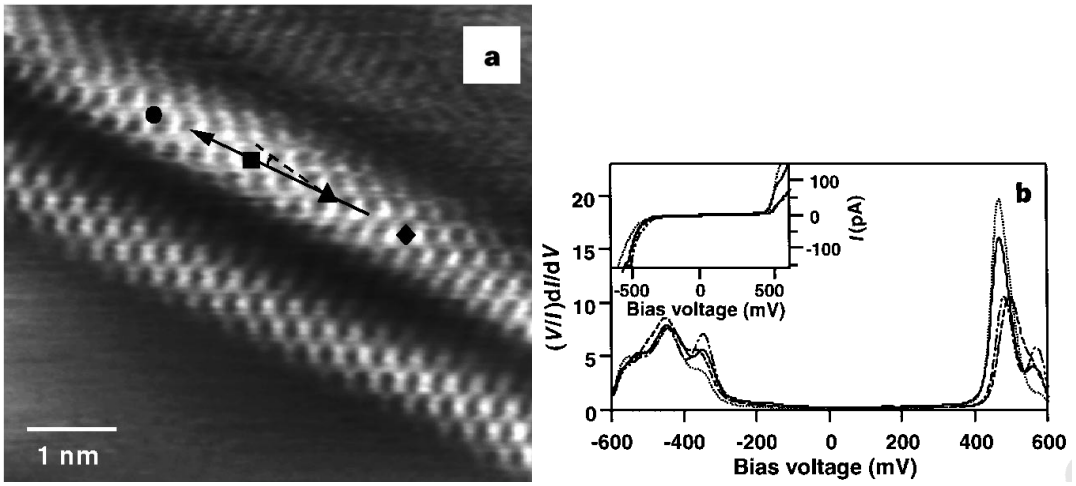

Figure 4: (a) Scanning tunneling microscope image of isolated single-walled nanotubes. As mentioned in the reference below, the black arrow highlights the tube axis, and the dashed line indicates the zigzag direction. (b) Plot of the normalized conductance and I–V values (inset) measured at the four locations marked in the carbon nanotube in (a). Reprinted with permission from T. W. Odom, J.-L. Huang, P. Kim and C. M. Lieber, Nature **391**, 62 (1998). Copyright 1998 Macmillan Magazines Limited.

nonvanishing within the gap, but this may be explained by the existence of tunneling through the nanotube to the gold substrate.

The majority of the measurements reported in Refs. [35] and [36] have determined the existence of moderate gaps, consistent with the geometric structure of semiconducting nanotubes. The experimental observations of the gap Δ fit very well to the dependence on the diameter given on theoretical grounds by Eq. (7). The parameter t which gives the best fit is very close to the nearest-neighbor overlap energy obtained from calculations in a single graphene sheet, $t = 2.5$ eV [42].

In the rest of the instances, the measurements of the differential conductance have not shown peaks in the spectra over a wider range of energies, larger than 1.5 eV. The manifest nonvanishing value of the conductance, together with its smooth behavior, is the signature of the metallic character in the nanotubes. When this happens, the geometric structure of the nanotubes has been shown to correspond either to armchair nanotubes or to chiral nanotubes with the helicity suitable for metallic behavior. It has been mentioned above that, in the latter case, a small gap, of the order of ~ 0.01 eV, should open at the Fermi level by effect of the curvature of the nanotube. Such a gap, however, has been only observed through high-resolution measurements of the conductance in zig-zag nanotubes of $(3n, 0)$ type[43]. It is believed that, in the case of the chiral nanotubes of $(3n + m, m)$ type, the small-gap feature tends to be even tinier[44] and its observation may be then precluded by the instrumental noise.

The use of tunneling spectroscopy has given then important information about

the band structure of the carbon nanotubes. It has shown that they can be considered as molecular wires. The proportion of the semiconducting nanotubes in the whole set considered in the experiments seems to agree with the ratio of two thirds predicted from pure theoretical arguments. Another important point is that the measures taken on metallic nanotubes in a rope are similar to those on isolated metallic nanotubes, as reported in Ref. [36], what seems to imply a weak intertube coupling of the nanotubes within a rope.

The fact that a slight variation in the geometric structure of a carbon nanotube may produce important changes in the conducting properties opens the possibility to build metal/semiconductor or semiconductor/semiconductor junctions in a single molecule. This requires changing the helicity within the same carbon nanotube, which can be achieved by introducing topological defects like combinations of heptagon and pentagon carbon rings in the nanotube lattice[21, 22, 23]. A pentagonal ring induces some local curvature in the hexagonal lattice, which can be superposed on a plane and has therefore no intrinsic curvature. The curvature of the pentagonal ring has to be counterbalanced with the opposite induced by an heptagonal ring in order to recover the tubular structure.

The combination of adjacent pentagonal and heptagonal rings has been proposed in Ref. [21] to produce changes in the chirality of a nanotube from a (n, m) structure to another of $(n \pm 1, m \mp 1)$ type. The particular case of a junction between $(8, 0)$ and $(7, 1)$ nanotubes has been analyzed, studying in detail the change in the band structure across the interface. This would be a typical instance of semiconductor/metal junction, and the evolution of the gap along the nanotube has been established theoretically by computing the local density of states. The example of a semiconductor/semiconductor junction formed by $(8, 0)$ and $(5, 3)$ nanotubes has been also studied, stressing the appearance of interface states in the gap from the presence of three pentagon-heptagon defects[21].

Experimental observations of the carbon nanotube intramolecular junctions have been already carried out[10, 45]. In the experiments reported in Ref. [45], the atomic structure of the nanotube segments at each side of the junction has been resolved by using scanning tunneling microscopy. This has made also possible to study the evolution through the junction of the different features in the local density of states. On the other hand, the experiments presented in Ref. [10] have investigated the peculiar transport properties of the intramolecular junctions.

In atomic force microscope images, the intramolecular junctions appear as kinks in individual carbon nanotubes, as illustrated in Fig. 5 taken from Ref. [10]. The large angle formed by the two segments at each side of the junction requires that the heptagon and pentagon rings are located at opposite sides of the nanotube section. By employing the electrodes shown in the figure, it has been characterized that the nanotubes in Fig. 5(a) give rise to a metal/semiconductor junction, while those in Fig. 5(b) provide an example of metal/metal junction[10].

The conductance through the kink is very different for the two samples shown in Fig. 5. In the sample shown to the left, the resistance at zero bias voltage is extremely large, higher than 250 GΩ[10]. The current I measured as a function of the bias voltage V (I–V characteristics) displays a highly nonlinear behavior. With

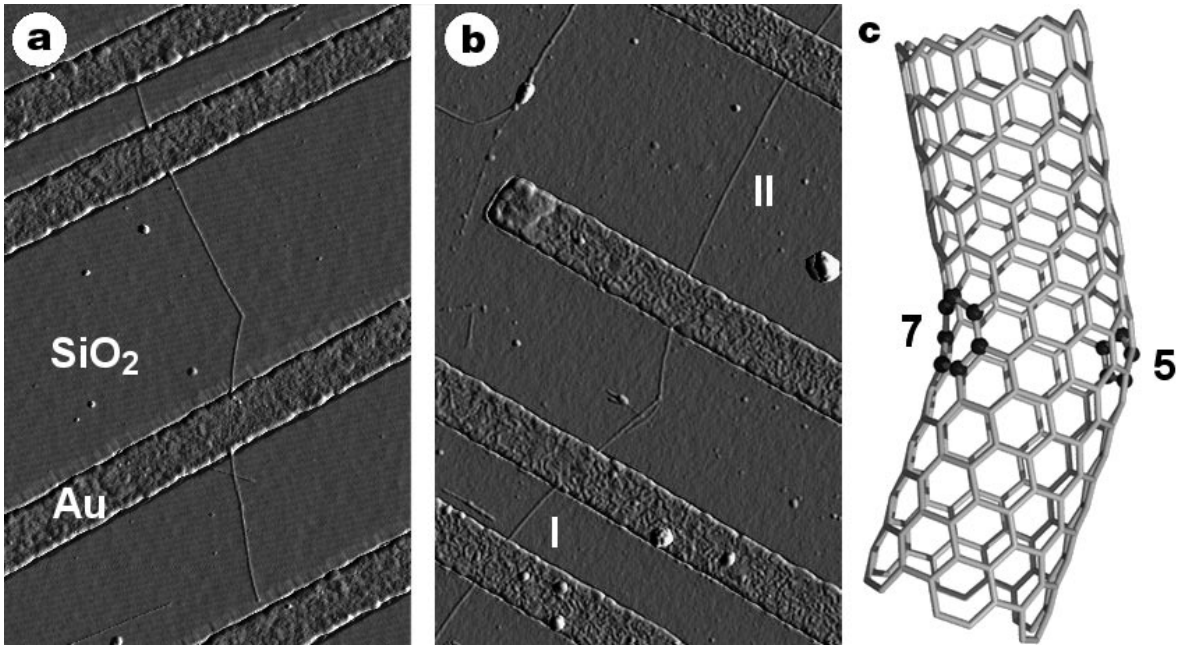

Figure 5: (a),(b) Atomic force microscope images of intramolecular junctions of carbon nanotubes. The pads seen in the figures correspond to titanium-gold electrodes embedded in the SiO_2 substrate, with the nanotubes placed on top of them. (c) Model of a kink created by the combination of the pentagonal and the heptagonal ring marked in the figure, and that gives rise to a junction between armchair and zigzag nanotube geometries. Reprinted with permission from Z. Yao, H. W. Ch. Postma, L. Balents and C. Dekker, Nature **402**, 273 (1999). Copyright 1999 Macmillan Magazines Limited.

no voltage applied to the gate, the current shows a small increase when a negative bias voltage is applied to the electrodes, while it shows a sharp increase for a positive voltage above 2 V (applied to the upper electrode)[10]. The kink induces therefore a rectifying behavior in the current, which has led to propose that it could be used as a molecular device resembling a diode. It has been stressed in Ref. [10] that the $I - V$ characteristics become more asymmetric as a gate voltage is applied to the substrate. This has been presented as an evidence that the lower segment of the nanotube in Fig. 5(a) is semiconducting. The upper segment is metallic in any event, since its resistance of 110 kΩ (measured at room temperature) does not show dependence on the gate voltage[10].

It has been established that the kink in Fig. 5(b) produces a metal/metal intramolecular junction[10]. The behavior of its conductance, however, cannot be understood in the framework of the single-electron picture described above, which does not take into account the effects of the Coulomb interaction. This leads to a strong correlation between the electrons in materials with reduced dimensionality. The features introduced by the electron-electron interaction in the behavior of the carbon nanotubes are reviewed in the sections below.

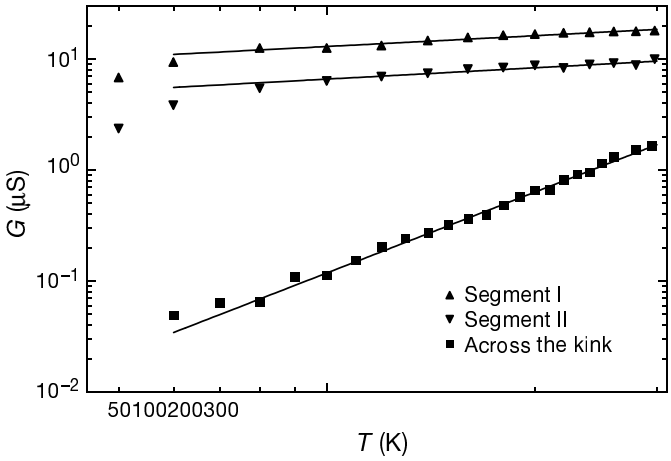

Figure 6: Log-log plot of the temperature dependence of the conductance, measured in the two nanotube segments and through the kink shown in Fig. 5(b). The straight lines correspond to the best fit to a power law for each set of data. Reprinted with permission from Z. Yao, H. W. Ch. Postma, L. Balents and C. Dekker, Nature **402**, 273 (1999). Copyright 1999 Macmillan Magazines Limited.

3 Transport properties of carbon nanotubes

3.1 Luttinger liquid behavior

The metallic carbon nanotubes show transport properties that deviate remarkably from those of the conventional two and three-dimensional metals. This is actully a consequence of their behavior as genuine one-dimensional conductors. Their transport properties cannot be understood from the standard Fermi liquid picture for interacting electrons, in which it is assumed that the elementary excitations are quasiparticles which behave similarly to free electrons, with just some characteristic parameters (like the effective mass) renormalized by the interaction. The failure to apply that Fermi liquid picture already anticipates the kind of exotic effects that may be found in molecular electronics, as well as it was anticipated on theoretical grounds many years ago that a new paradigm —the Luttinger liquid— should be used to describe the interacting electrons in one-dimensional systems[46, 47].

The observation of unconventional transport properties has been reported in Ref. [10], for instance, regarding the sample shown in Fig. 5(b). The two-terminal conductance G as a function of the temperature is represented in Fig. 6, from the mentioned reference, where it can be appreciated the behavior in the two different segments and through the metal/metal junction. It is remarkable the strong suppression of the conductance as the temperature decreases in the latter case. In all the instances, the behavior can be fitted very well by a power-law dependence $G(T) \propto T^{\alpha}$ in a fairly large range of temperatures. The exponents corresponding to the upper and the lower segment of the sample are $\alpha = 0.34$ and 0.35, respectively, and the value obtained through the kink is $\alpha = 2.2$.

As remarked by the authors of Ref. [10], the fact of producing contacts between the electrodes and the nanotube with sufficiently low resistance (about or smaller than 100 kΩ in their experiment) seems crucial to observe a definite behavior of the conductance. The suppression for decreasing temperature could be attributed, in principle, to activated transport over the tunnel barrier created by each contact. This would lead, however, to a dependence $G(T) \propto \exp(-\Delta/k_B T)$, in terms of the barrier height Δ, which cannot fit well the experimental data. The measurements of the conductance refer therefore to a property intrinsic of the carbon nanotube. This has to do with the effects of the electronic interaction, since the large suppression of the conductance through the junction cannot be accounted for by a model of noninteracting electrons with topological defects[48].

The behavior of the tunneling conductance is actually related to that of the density of states $\rho(E)$ at energies close to the Fermi level. It will be shown below that the density of states has a power-law dependence $\rho(E) \propto E^\alpha$ in the framework of the Luttinger liquid theory, with the exponent α being a function of the interaction strength[46, 47]. The fact that $\rho(E)$ goes to zero at the Fermi level is a consequence of the absence of low-energy excitations with the properties of noninteracting electrons. The observation of the power-law dependence of the tunneling conductance can be considered then as another manifestation of the carbon nanotubes as genuine one-dimensional conductors.

The data in Fig. 6 show that the Luttinger liquid behavior may extend over a wide range of temperatures, up to 300 K. At sufficiently low temperatures, the power-law behavior of the tunneling conductance is modified by the effect of the Coulomb blockade[49], which is also described below in detail. That effect is observable in the experiments when the thermal energy (i.e. the temperature times the Boltzmann constant k_B) becomes low enough to be comparable to the discrete energy needed to put one more electron on the finite dimensions of the system. This quantity is the so-called charging energy E_c, which is given in terms of the electron charge e and the total capacitance C of the nanotube by the expression $E_c = e^2/2C$. The charging energy can be estimated as a few meV in the typical single-walled nanotubes (with lengths of the order of 1 μm) used in the experiments.

Evidence of power-law behavior has been also obtaind from the measurements of the differential conductance dI/dV, in individual single-walled nanotubes[10] as well as in ropes of nanotubes[50]. Fig. 7 illustrates the results of the experiments in ropes reported in Ref. [50]. For values of the bias voltage applied to the rope such that $eV \ll k_B T$, the effect of the temperature prevails and the differential conductance recovers the voltage-independent value given by $G(T)$. At higher bias voltage, the experimental values of dI/dV show a well-defined linear behavior in log-log scale as a function of the bias voltage at different temperatures. The exponent giving the best fit for the power-law dependence $dI/dV \propto V^\alpha$ is $\alpha = 0.36$ [50]. It is also remarkable that, upon scaling of the differential conductance by the values of T^α as dictated by the behavior of a tunnel junction[51, 52], the experimental data for the different temperatures fall into a unique universal curve when represented as a function of the scaled variable $eV/k_B T$ [50].

The exponents obtained for the transport through the tunnel junctions created by

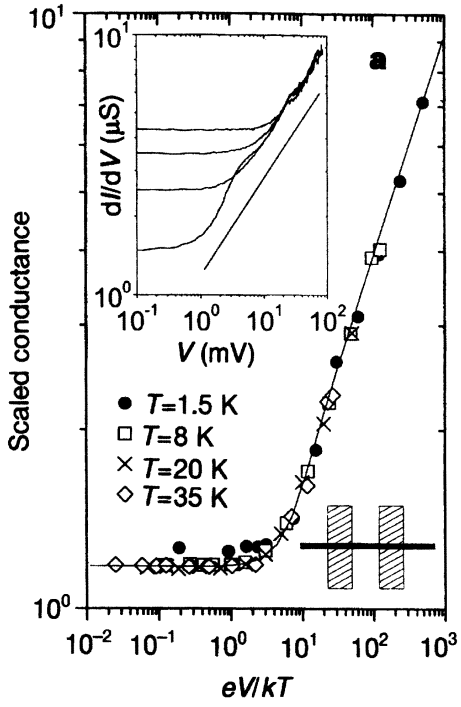

Figure 7: Log-log plot of the differential conductance in a rope, measured at different temperatures and scaled by T^{α} in each case. The inset shows the curves of differential conductance as a function of the bias voltage, for decreasing values of the temperature (from top to bottom). Reprinted with permission from M. Bockrath, D. H. Cobden, J. Lu, A. G. Rinzler, R. E. Smalley, L. Balents and P. L. McEuen, Nature **397**, 598 (1999). Copyright 1999 Macmillan Magazines Limited.

the contacts in the ropes and in the individual nanotubes are in very good agreement. From this fact, one can obtain significant information about the physical properties of the ropes. The agreement is consistent, for instance, with the results establishing the large suppression of the tunneling amplitude between the different nanotubes of a rope[53, 54]. This means that the only relevant intertube coupling arises from the Coulomb interaction. Consequently, it can be concluded that the transport properties measured in individual nanotubes as well as in ropes are dominated by the two tunnel junctions in the circuit, which give rise to the observed power-law behavior. In the measurements through the kink reported in Ref. [10], the reason for the enhanced decrease of the conductance has to be found in the additional suppression of the tunneling of electrons between the two ends of the nanotube segments, according to the Luttinger liquid picture.

From a theoretical point of view, the clarification of the Luttinger liquid behavior of the metallic carbon nanotubes has been accomplished in Refs. [55] and [56]. The analyses carried out there assume that the repulsive Coulomb interaction between electrons is dominant in the single-walled carbon nanotubes. The discussion focuses on the low-energy regime in which only the four linear branches near the Fermi level (as observed in the band structure of Fig. 3 for instance) contribute to the electronic

properties. When two electrons interact in the nanotube, there is a large number of possible processes, which can be classified depending on whether the electrons scatter near the same Fermi point or not, or whether the electrons shift from one Fermi point to the other. One of the main conclusions drawn in Refs. [55] and [56] is that the processes in which the electrons remain in their respective linear branches after scattering are largely dominant. The interaction strength of the rest of processes (the so-called backscattering and Umklapp interactions) is suppressed in general by a factor inversely proportional to the number of subbands in the nanotube[55, 56].

The hamiltonian H governing the low-energy electron dynamics can be approximated then by writing the interactions of the form density times density which arise from the Coulomb repulsion,

$$\begin{aligned} H &= \frac{1}{2}\hbar v_F \int dk \sum_{r\sigma} \rho_{r\sigma}(k)\rho_{r\sigma}(-k) \\ &\quad + \frac{1}{2}\int dk \sum_{r,s,\sigma,\sigma'} \rho_{r\sigma}(k)\ V(k)\ \rho_{s\sigma'}(-k) \end{aligned} \tag{9}$$

$\rho_{r\sigma}(k)$ being the electronic density in the linear branch r for spin σ, and $V(k)$ being the Fourier transform of the Coulomb potential. The kinetic term in (9) gets the appropriate dimensions from the Fermi velocity v_F of the electrons and the Planck constant $\hbar (= h/2\pi)$.

In one spatial dimension, the density operators can be rescaled to satisfy canonical commutation relations characteristic of boson operators[46, 47]. The hamiltonian (9) can be diagonalized in terms of these bosonic objects. For this reason, the states with well-defined energy do not correspond to the original electrons, but to collective excitations that represent physically wave-like modulations of charge or spin.

The transformation diagonalizing the hamiltonian (9) is a pseudorotation determined by the parameter $\mu = 1/\sqrt{1 + 8V/\hbar v_F}$ [46, 47], where a suitable average value of the interaction strength V is assumed. All the properties of the Luttinger liquid are completely characterized by the parameter μ. Thus, the density of states $\rho(E)$ follows at low energies the power-law behavior

$$\rho(E) \propto E^{\alpha} \tag{10}$$

with an exponent $\alpha_{\rm bulk} = (\mu - \mu^{-1} - 2)/8$ for the density of states measured in the bulk of the liquid[55, 56]. In the case of an open one-dimensional system, the density of states is substantially smaller at the ends of the liquid, having then a power-law behavior with an exponent $\alpha_{\rm end} = (\mu^{-1} - 1)/4$ [56].

From the measurements of the conductance when tunneling into the bulk of the nanotube, it turns out that the best fit of the experimental data corresponds to a Luttinger liquid parameter μ around 0.22 [10]. This is the signature of a significant electron-electron repulsive interaction in the single-walled nanotubes, and indeed that value for μ agrees well with the theoretical estimate obtained by assuming that the Coulomb interaction is dominant in the individual nanotubes[55, 56]. An important consistency check is that the exponent that can be predicted for the tunneling

into the end of the nanotube accounts for the large suppression of the conductance through the kink observed in Ref. [10]. Taking $\mu \approx 0.22$, the exponent $\alpha_{\rm end}$ becomes ≈ 0.9. For the tunneling through the metal/metal junction, the conductance has to be proportional to the product of the tunneling density of states at each end of the nanotube segments. Thus, the corresponding exponent has to be twice the value of $\alpha_{\rm end}$, which is close to the estimate (≈ 2.1) from the fit of the experimental data[10]. Overall, there is therefore strong evidence that the Luttinger liquid picture applies to the tunneling processes in the single-walled nanotubes.

3.2 Ballistic transport properties

The experimental signatures of Luttinger liquid behavior are consistent with another remarkable observation in the carbon nanotubes, as it is the ballistic transport. This means that the charge can move along the nanotube in such a way that it is not disturbed by inelastic collisions. This behavior as a quantum conductor is opposite to the classical behavior in which the conduction takes place by diffusion of the electrons with a certain mean free path. One of the consequences of ballistic transport is that there cannot be dissipation of energy inside the ballistic conductor, and that the heat produced has to appear at the leads of the ballistic element. Moreover, another important property is that the conductance has to be quantized in units of $G_0 = 2e^2/h$, with each mode in the waveguide contributing with one of these quanta to the conductance[57, 58, 59].

The quantization of the conductance has been observed at room-temperature in fibers of multi-walled nanotubes. The peculiarity of the experiment reported in Ref. [7] is that the fibers have been used in place of the tip of a scanning probe microscope. This has allowed to raise and lower the fiber inside a liquid metal, used as a second contact to close the circuit. By dipping the fiber into the metal, the current has been recorded as a function of the length of the fiber within the liquid. This has shown that the conductance increases by steps whose magnitude is very close to the quantum of conductance $G_0 = 2e^2/h$. The appearance of each step corresponds to the point at which one more multi-walled nanotube becomes in contact with the liquid metal[7].

The measurements reported in Ref. [7] provide a strong indication of ballistic transport in the multi-walled samples, since they have shown that the conductance does not decay over a variation of about 200 nm of the nanotube length submerged in the liquid. Supporting the same conclusion, there is also evidence that the heat produced by the current cannot be dissipated in the nanotubes. It has been estimated in Ref. [7] that the current densities produced in the experiment can be higher than 10^7 A cm^{-2}. These values are so large that, if the corresponding dissipation of energy had to take place within the fiber, it would give rise to a temperature well above that needed to burn the nanotubes[7].

The quantization of the conductance in the multi-walled nanotubes also sheds light on their internal structure. Each individual metallic nanotube has two modes contributing to the conduction properties, irrespective of the diameter of the tubule. This means that each metallic shell of a multi-walled nanotube could in principle

contribute with two quantum units to the conductance, what is not observed in the experiment of Ref. [7]. This can be explained by the fact that only the outer shell participates in the conduction, what is plausible since, even in the event that the next layer were metallic, the resistivity in the direction perpendicular to the tubules has to be very large[3]. It still remains to be understood why the step observed in the conductance is given by G_0, instead of $2G_0$. This value accounts for the contribution of the two spin projections and the two propagating modes of the nanotubes, what suggests that the contribution of some of these degrees of freedom may be missing in the multi-walled samples[60].

The observation of ballistic propagation seems to require very pure nanotube samples and, indeed, there is evidence of the structural perfection of the multi-walled nanotubes used in the experiments of Ref. [7]. When the degree of purity is not so high, the ballistic propagation may be altered by the interactions with the impurities or defects in the samples. In the experiments presented in Ref. [61], for instance, the transport properties of several single-walled nanotubes with large intrinsic resistance have been measured, showing a highly nonlinear behavior upon variation of the length along the nanotube. For a separation between the contacts of the order of a few hundred nanometers, the resistance displays a very smooth dependence on the length of the nanotube segment. This has been interpreted as the signature of ballistic transport in the single-walled nanotubes[61]. Over larger distances, the resistance shows a steep increase, which is incompatible with Ohm's law in any event since this would imply a linear dependence of the resistance on the length of the wire. It has been argued that the overall behavior can be only consistent with a situation in which the transport is dominated by the elastic scattering with an increasing number of defects, which would give rise to the observed decrease of the probability amplitude over the length of the nanotube[61].

3.3 Low-temperature properties

In a different kind of experiments, it has been established that the electron wave-functions can be extended over lengths of several microns in the single-walled nanotubes, when the contitions are such that the thermal energy is smaller than the single-particle level spacing in the tubes[4, 5]. These low-temperature experiments are measuring therefore a regime different to that probed by the experiments reporting the Luttinger liquid behavior, where the interaction between a manifold of single-particle levels is manifest.

The separation ΔE between the single-particle energy levels is dictated by the length L of the nanotube according to the expression

$$\Delta E = h v_F / 2L \tag{11}$$

where v_F is the Fermi velocity ($\approx 8 \times 10^5$ m s^{-1}). For typical lengths of a few microns, the separation between the discrete energy levels is below 1 meV. When the thermal energy is below that value, single electrons can be added to the nanotube by resonant tunneling, that is by adjusting the bias voltage applied to the leads so that the current increases by one step each time that a new molecular orbital

becomes available[5]. Similarly, a series of sequential peaks can be observed in the conductance when the number of electrons is varied with the voltage applied to the gate[4]. The fact that the single-particle level splitting can be resolved by looking at the current steps working at suitably low temperatures is the signature that the electrons occupy molecular orbitals that correspond to delocalized electronic states.

Moreover, direct evidence of the extended character of the electron states has been obtained by imaging the electron wavefunctions in short nanotubes (with length $L \approx 30$ nm) by scanning tunneling microscopy[62]. By measuring the tunneling conductance along the nanotube, it has been observed the spatial modulation corrresponding to the electron probability amplitude, finding agreement with the expected wavevectors of the quantized states in the nanotube. The electron wavefunctions of several discrete molecular levels have been discerned with this technique[62].

Another remarkable observation, related to the existence of extended electron wavefunctions, refers to the oscillatory behavior of the magnetoresistance of multi-walled nanotubes[63]. When these are aligned with the direction of the magnetic field, it has been shown that the resistance has modulations as a function of the enclosed flux. This is consequence of the fact that the phase of the electron wavefunction is modified by the presence of the magnetic field (the so-called Aharonov-Bohm effect). When the electrons encircle the nanotubes in opposite directions, a phenomenon of quantum interference takes place, which reflects in the behavior of the resistance[63].

The absence of localization of the electronic states in the single-walled nanotubes may be surprising at first sight. On the one hand, there is the well-known fact that a single impurity has the ability to disrupt the conduction in a one-dimensional system[64, 65]. It has been shown, however, that the case of the nanotubes is special as the electrons feel the effect of impurities averaged over the circumference of the tube[66]. Thus, the metallic nanotubes may have very good conduction properties, with delocalized states over lengths of 10 μm or more for the nanotubes produced in the experiments. Furthermore, that localization length has to be an increasing function of the diameter of the nanotube[66].

The picture that emerges from the low-temperature experiments on transport is that the quality of the contacts used for the nanotubes determines the type of experimental observation. In some metallic nanotube devices, the resistance measured at room-temperature is close to the theoretical lower limit of ≈ 6.5 kΩ, given by the inverse of the conductance $2G_0$ that would correspond to two modes propagating ballisticaly along a single-walled nanotube. In these cases, most part of the resistance has to be attributed to the nanotube, while the contacts between the metallic electrodes and the nanotube are nearly perfect. At low enough temperatures such that the thermal energy is below the single-particle level spacing within the nanotube, the electrons pass through the interface with little reflection and the experimental observations account for the propagation intrinsic to the nanotubes.

In the experiments reported in Ref. [6], a number of nanotube devices were measured with room-temperature resistances below 15 kΩ. In these samples the average value of the conductance has been found always between G_0 and $2G_0$, the departure from the latter value being attributed to the scattering of the electrons at

the nanotube-electrode interface. Moreover, the two-dimensional plot of the differential conductance dI/dV as a function of the bias voltage V and the gate voltage V_g displays a quasiperiodic pattern of dips and peaks. It has been shown that the oscillation period scales appropriately with the inverse of the nanotube length, what supports that the observed pattern is due to the quantum interference of the electron waves after being scattered at the interfaces[6]. This shows the significance of taking into account the quantum coherence, represented by the extended character of the electron wavefunction, when designing low-temperature electronic devices at the molecular level.

Opposite to the cases of devices with almost transparent contacts, there are instances where the transmission between the nanotube and the metallic leads is dominated by much more suppressed tunneling processes. In these cases, the experimental observations give a measure of the difficulty that the current finds to go through the tunnel junction. In certain circumstances, it is possible to control the tunneling of single electrons into the nanotube, entering a regime with new physical properties which is described in the next section.

4 Coulomb blockade and quantum dot behavior

4.1 Carbon nanotubes as single-electron transistors

One of the main interests in the technological application of the carbon nanotubes arises from the possibility of developing electronic devices made of a single molecule. Semiconducting nanotubes have been proposed to act as field-effect transistors in Refs. [11] and [12]. In these devices, source and drain electrodes are attached to the semiconducting nanotube, while this is separated from the substrate (the gate electrode) by an oxide layer which acts as a dielectric. The capacitive coupling between the nanotube and the substrate is what makes possible to change the density of charge carriers and the conduction properties in the nanotube by varying the voltage of the gate.

Unlike field-effect transistors, however, single-electron devices are based on the intrinsic quantum-mechanical character of the tunnel effect. In the case of metallic nanotubes, the development reported in Ref. [14] is that the electrons can be confined in short islands between two buckles of the tubule, so they can be added one by one by suitable variations of the voltage applied to the external gate.

The technique applied in Ref. [14] consists of using the tip of an atomic force microscope to press the nanotube against the substrate. The tip is then moved until the nanotube is strongly bent. In this way a buckle is created in the tubular structure, leading to a tunnel barrier for electron transport in a metallic nanotube. Two of these buckles can be arranged in series in an individual metallic nanotube, in order to study the transport properties through the two tunnel barriers[14]. One of the structures which have been produced with this technique can be observed in Fig. 8. The short nanotube segment that appears there between the buckles has a length of the order of 25 nm.

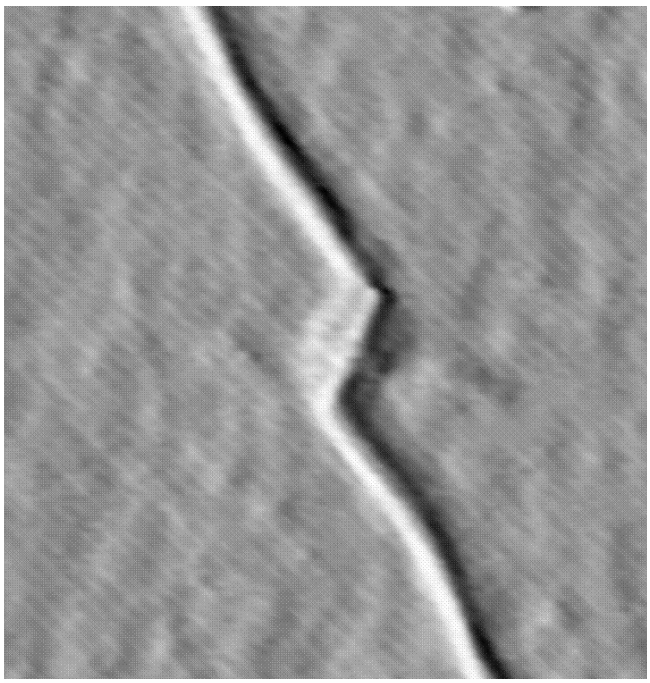

Figure 8: Atomic force microscope image of a short nanotube island between two buckles, formed by manipulation with the atomic force microscope tip. Image courtesy of Cees Dekker, Delft University of Technology.

When the tunneling of the electrons takes place into a short nanotube island, it costs a relatively large energy to add a single electron between the tunnel barriers. This is the well-known effect of Coulomb blockade[49]. On the one hand, there is the energy needed to overcome the electrostatic repulsion between the electrons which are confined in such a reduced dimension, the so-called charging energy E_c. As pointed out above, this is given by the expression $E_c = e^2/2C$, in terms of the total electrostatic capacitance C [49]. On the other hand, each new electron added is placed in the first unoccupied level, what requires to spend an energy corresponding to the separation ΔE between quantized levels. That energy difference is inversely proportional to the length L of the island, according to the already quoted expression $\Delta E = hv_F/2L$ (or $\Delta E = hv_F/4L$ if the degeneracy between the two different low-energy modes in the metallic nanotubes has been lifted). Altogether, the energy needed to add an electron to the island is the sum of the two contributions, the so-called addition energy[67]

$$E_{\rm add} = e^2/C + \Delta E \tag{12}$$

For the short nanotube segments created with the technique reported in Ref.

[14], the charging energy and the level spacing ΔE have comparable magnitudes, and they give rise to an addition energy $E_{\rm add}$ of the order of 0.1 eV, which is considerably larger than the thermal energy $k_B T$ at room temperature. For that reason, the transport properties resulting from the addition of single electrons to the island can be observed without resorting to the use of low temperatures. The number of electrons transferred between the two buckles is controlled by varying the gate voltage applied to one of the substrates, capacitively coupled to the nanotube, what allows to lower the successive empty energy levels of the nanotube island down to the Fermi level in the outer nanotube segments[14].

The single-electron transport properties are distinctively observed in the measurements of the differential conductance dI/dV through the tunnel barriers reported in Ref. [14]. The effect of Coulomb blockade gives rise to typical patterns in the intensity plot of the differential conductance as a function of the bias voltage V applied to the electrodes and the voltage V_g applied to the external gate. At fixed gate voltage, a gap can be generally observed in the measures of dI/dV as a function of the bias voltage, corresponding to the region where that is not large enough to reach the first unoccupied level within the island. At some values of V_g the gap closes, what marks the points at which the first empty level in the region between the tunnel barriers is aligned with the Fermi level outside the island. This produces a typical pattern of consecutive diamond-like regions with suppressed conductance in the intensity plot of the differential conductance in the (V_g, V) plane[14].

An illustration of the diamond-shaped regions (although corresponding to a different experiment reported in Ref. [68]) is given in Fig. 9. The dark diamonds correspond to the regions where the differential conductance is suppressed. In each diamond the number of electrons in the nanotube segment is fixed, while it increases by one unit when shifting from a diamond to the next one. On the other hand, the addition energy $E_{\rm add}$ can be obtained from the height in bias voltage of the largest diamond, since that is the voltage required to establish the conduction through the nanotube segment. In the case of the short island of Ref. [14], the addition energy is $E_{\rm add} \approx 120$ meV. The separation of the energy levels has been estimated as $\Delta E \approx 38$ meV, from where a value $E_c \approx 41$ meV has been obtained for the charging energy of the short island[14].

It turns out that, for the nanotube device described in Ref. [14], the level separation ΔE and the charging energy E_c have comparable magnitudes, and both of them are well above the thermal energy $k_B T$ corresponding to room temperature. The behavior of the conductance at lower temperatures has been also studied in Ref. [14], reaching another important conclusion. The conductance of the nanotube follows a clear power-law dependence with decreasing temperature, pointing at a Luttinger liquid behavior of the kind already observed in Refs. [10] and [50]. It has been remarked that the exponents measured for that dependence do not correspond to a picture in which the transport proceeds with the sequential, independent tunneling through the two barriers that form the nanotube device. Instead, it has been shown that the data can be fitted with the exponent appropriate for correlated tunneling, in which the electrons propagate coherently through the nanotube island[14]. The corresponding value found for the parameter measuring the interaction strength,

$\mu = 0.23$, is in very good agreement with the earlier estimates from Luttinger liquid behavior in carbon nanotubes[10, 50].

4.2 Quantum dot behavior

Effects related to the confinement of the electrons in a reduced dimension have been also observed in multi-walled nanotubes. In this case, the experiments reported in Ref. [68] have been realized at temperatures reaching values down to 280 mK. Such small temperatures are needed to discern charging energies and single-particle level spacings which range below 1 meV for multi-walled nanotubes with typical lengths of a few microns.

The experimental measurements of the differential conductance carried out in Ref. [68] are represented by the intensity plot of Fig. 9. The dark regions correspond to lower values of the differential conductance, and it can be clearly seen that they form a sequence of diamonds as the gate voltage increases. There seems to be periodicity in the pattern formed by a large diamond and three consecutive smaller ones. Recalling that the number of electrons in the nanotube is increased by one unit from one diamond to the next and that the height of the diamond gives the energy required to add one electron, the observed pattern points at a four-fold degeneracy of the electronic levels in the multi-walled nanotube[68]. The height of the large diamond should correspond to the addition energy $E_{\rm add} = e^2/C + \Delta E$, as in the measurement of the short island reported in Ref. [14]. The size of the smaller diamonds should give a measure of the charging energy alone, with the electrons being placed there in the same single-particle level[68].

The four-fold degeneracy is in agreement with the expected band structure of a metallic nanotube, in which two subbands cross at the two Fermi points of the one-dimensional structure. It may be surprising, however, to find that only two gapless modes contribute to the conduction properties in the multi-walled nanotubes. In general, these are significantly hole doped by the environment, and the Fermi level in the outermost tubule crosses several different subbands[69]. It may well happen to have an outer shell which is semiconducting, so that for appropriate choices of the gate voltage it may not contribute to the conductance of the multi-walled nanotube. As explained in Ref. [68], this seems to be the case of the experimental sample exhibiting the sequence of diamonds in the differential conductance. It has been observed that such a sequence appears for suitably large values of the gate voltage. According to the arguments given in Ref. [68], the features observed in the conductance should reflect the metallic properties of the tubule next to the outermost shell, as that nanotube would not be affected by the external doping.

As remarked above, the height of the smaller diamonds in the intensity plot of the differential conductance gives a measure of the charging energy E_c. For the multi-walled nanotube sample considered in Ref. [68], the estimate is $E_c \approx 0.4$ meV. From the value of the addition energy, it turns out that $\Delta E \approx 0.8$ meV [68]. As explained in the preceding section, the level spacing arises from the quantization of the electron states in the finite length of the nanotube. It has been observed in Ref. [68] that the estimated value of ΔE corresponds to the propagation along

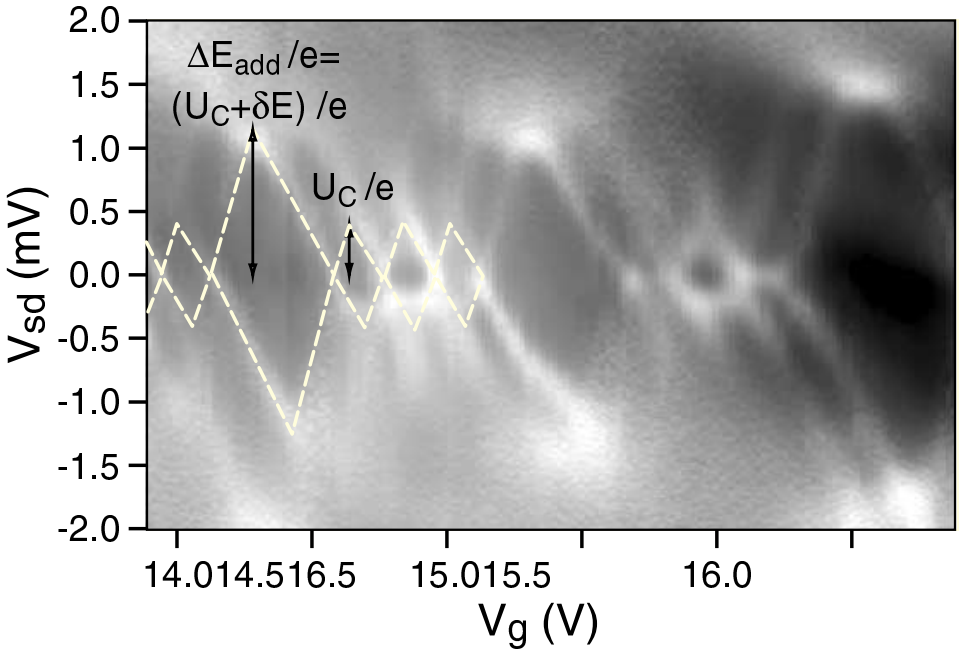

Figure 9: Intensity plot of the differential conductance of a multi-walled nanotube as a function of the bias voltage V_{sd} and the gate voltage V_g. The average conductance is of the order of $\sim 2e^2/h$. According to the reference below, ΔE_{add}, U_c, and δE denote the addition energy, the charging energy, and the single-electron level spacing, respectively. Reprinted from M. R. Buitelaar, A. Bachtold, T. Nussbaumer, M. Iqbal and C. Schönenberger, Phys. Rev. Lett. **88**, 156801 (2002). Copyright 2002 by the American Physical Society.

the whole length of the nanotube (≈ 2.3 μm), rather than to the distance between the electrodes (≈ 300 nm). It has been argued that this further supports the idea that the outermost shell does not participate in the conduction of the multi-walled nanotube[68]. The quantization properties over the nanotube length show, as well as in the individual single-walled nanotubes, that the electron wavefunctions can be extended over large distances (above ~ 1 μm) due to the weak influence of disorder with increasing diameter size[66].

Another physical effect reported in Ref. [68] refers to the behavior of the spin of the states with different electron number. By studying the behavior of the conductance under a magnetic field perpendicular to the tubules, it has been found that the spin follows the sequence $1/2, 0, 1/2, 0 \ldots$, upon adding one more electron each time to the nanotube. This can be explained if pairs of electrons have antiparallel spins, leading to the change from spin 1/2 for an odd number of electrons to a vanishing value for an even number[68]. In general, the Coulomb repulsion between two electrons is minimized if they can be placed in degenerated orbitals, allowing them to have parallel spins[70]. This rule is not followed in the the multi-walled nanotube considered in Ref. [68], what has been interpreted there as a signal that the perfect degeneracy between the modes of the two low-energy subbands in a metallic

nanotube is spoiled in the experimental sample.

Moreover, it has been found in Ref. [68] that the differential conductance increases in the regions with an odd number of electrons as the temperature decreases below 1 K. This has been regarded as a manifestation of the Kondo effect, which deals in general with the properties of a static spin surrounded by delocalized electrons[71, 72]. In the Kondo system there is an energy scale, given by the so-called Kondo temperature, below which the itinerant electrons are able to screen the static spin, with a concomitant increase of the conductance. The Kondo temperature gives therefore a measure of the binding energy of the singlet state formed by the screening effect. According to the authors of Ref. [68], the coupling between the spin of the nanotube and the electrons in the leads is what gives rise to the formation of the singlet state and the increase of the conductance through the nanotube.

The carbon nanotubes appear then as ideal systems to study the properties of electrons confined in a very reduced spatial dimension. This confinement into so-called quantum dots can be caused by the presence of the own electrodes acting as tunnel barriers. It has been also proposed that the arrangement of two consecutive kinks made from topological defects (i.e. from the combination of pentagon and heptagon rings) can be used to lock the electrons in short nanotube segments[73]. It has been already shown experimentally that the resonant electron scattering between simple (nontopological) defects gives rise to the formation of intratube quantum dots, with conductance patterns similar to that shown in Fig. 9 [74]. The charge states in the quantum dots can be actually imaged with scanned gate microscopy and electrostatic force microscopy, what may give interesting spatial information about the physical effects involved[75].

5 Superconducting correlations in carbon nanotubes

5.1 Proximity-induced superconductivity

There have been several experiments revealing the existence of superconducting correlations in the carbon nanotubes. These observations have taken the form of a drastic drop in the resistance of the nanotube samples below certain temperature. In one of the most remarkable experiments, reported in Ref. [76], it has been shown that a rope of carbon nanotubes is able to carry an electric current with zero voltage drop, when embedded between superconducting contacts. The measurement of that so-called supercurrent implies therefore a vanishing resistance of the conductor. The experiment provides a realization of the proximity effect, by which the electronic properties of a normal metal change drastically when placed in contact with a superconductor[77, 78]. In the latter, there is no sign of electron-like particles at low energies and, instead, a condensate formed by pairs of bound electrons is found[79]. These so-called Cooper pairs may extend their propagation to the nearby normal metal, giving rise to the electric current without dissipation of energy.

The influence of the superconducting electrodes in the electronic properties of single-walled nanotubes has been investigated in the experiments reported in Refs. [76] and [80]. One of the main differences between these experiments is that, in the

latter, the transport properties have been measured in a set of individual single-walled nanotubes. In the former experiment, the supercurrents have been observed in a massive rope made of about 200 nanotubes, and in a thin rope leading to a single nanotube at one of its ends. On the other hand, a common feature in both experiments is the low resistance attained for the samples that have shown the proximity effect. Typically the values measured at room temperature have been consistent with a resistance of the individual metallic nanotubes of the order or below the inverse of the conductance quantum, $h/e^2 \approx 25.8\ \mathrm{k}\Omega$ [76, 80]. Such values are comparable to the resistance $(2G_0)^{-1} = h/4e^2$ corresponding to the ballistic transport in individual nanotubes, what gives a measure of the high transparency of the contacts produced in the experiments.

In the experiments reported in Ref. [76], the ability to produce highly transparent junctions has been the result of using a remarkable technique allowing to suspend the nanotube ropes between the contacts. In the transport measurements, a drop to a vanishing resistance has been observed in the two nanotube samples mentioned above, below the temperature T_c of the transition of the electrodes to the superconducting state. The contacts were made of bilayer electrodes with respective temperatures $T_c \approx 1.1$ K for the Re/Au bilayer in the case of the thick rope, and $T_c \approx 0.4$ K for the Ta/Au bilayer in the case of the thin rope. By applying a magnetic field perpendicular to the nanotube axes, it has been possible to reduce the value of T_c as measured in the ropes, up to a point in which the transition disappears for a suitably large field[76]. This effect of the magnetic field is one of the genuine features of superconductivity, and it serves to corroborate the nature of the phenomenon observed in the experiment.

When increasing the current that flows along the rope, it can be supported without developing any resistance up to a maximum value, that is called the critical current. The behavior of the critical currents for the ropes studied in Ref. [76] has shown unconventional features, regarding their magnitude as well as their dependence with the temperature. The critical current should vanish for instance at the transition temperature of the contacts, but in the thick rope of Ref. [76] the behavior is very smooth instead near T_c. In the conventional picture of the proximity effect, the magnitude of the critical current should correspond to the expression $I_c = (\pi/2)\Delta/eR_N$, R_N being the normal state resistance and Δ the binding energy of the Cooper pairs in the superconducting condensate. As it has been pointed out in Ref. [76], the value of I_c estimated in that way is however 40 times smaller than what is actually measured in the thick rope. The thin rope shows a better agreement in the magnitude of the critical current, but this also displays a very unusual temperature dependence, with a flat behavior until the neighborhood of T_c is reached[76].

An explanation of the unconventional behavior of the critical currents in ropes has been presented in Ref. [81]. It has been shown the relevance of taking into account appropriately the interaction among the large number of metallic nanotubes that may be present in a rope. The Coulomb potential is not screened in an individual nanotube, but the interaction between the charges in different metallic nanotubes leads to a significant reduction of the effective interaction strength[81]. This can be

understood by thinking that, instead of (9), the hamiltonian appropriate for a rope with n metallic nanotubes is

$$\begin{aligned} H &= \frac{1}{2}\hbar v_F \int dk \sum_{ar\sigma} \rho^{(a)}_{r\sigma}(k)\rho^{(a)}_{r\sigma}(-k) \\ &+\frac{1}{2}\int dk \sum_{a,b,r,s,\sigma,\sigma'} \rho^{(a)}_{r\sigma}(k)\ V_{(a,b)}(k)\ \rho^{(b)}_{s\sigma'}(-k) \end{aligned} \tag{13}$$

the indices a, b labelling the charge densities in the different metallic nanotubes. The Coulomb interaction is long-ranged and takes place therefore between all of them, so that it contributes equally to all the $V_{(a,b)}(k)$ terms. The hamiltonian (13) can be diagonalized by passing to the total charge density $\rho_{r\sigma}(k) = \sum_a \rho^{(a)}_{r\sigma}(k)$. It becomes clear that the Coulomb interaction is only felt in the channel of the total charge, while there are still $n-1$ noninteracting partial channels[81].

The above argument explains that the repulsive electron-electron interaction becomes less relevant as the number n of metallic nanotubes increases in the rope. The proximity effect for a Luttinger liquid in contact with a macroscopic superconductor has been studied in Refs. [82] and [83], showing that the Cooper pairs propagate along the one-dimensional metal but giving rise to a supercurrent I_c that decays with the length L as

$$I_c \propto 1/L^{1/\mu} \tag{14}$$

where μ is the Luttinger-liquid parameter quoted above Eq. (10). Recalling that $\mu < 1$ in the case of a repulsive interaction, that kind of behavior can only account for the large critical current measured in the rope of Ref. [76] after the appropriate reduction in the strength of the Coulomb interaction is considered. It has been also shown in Ref. [81] that the temperature dependence of the critical currents can be reproduced by considering the one-dimensional propagation of the Cooper pairs, what gives further support to the picture of the single-walled nanotubes as genuine one-dimensional conductors.

In the experiment presented in Ref. [80], it has been measured the resistance of individual single-walled nanotubes placed between Nb electrodes. The nanotubes have been capacitively coupled to the Si substrate, and changing the gate voltage V_g has allowed to increase the already high transparency of the contacts. Below the transition temperature of the Nb electrodes ($T_c \approx 9.2$ K) and for some interval of V_g, a dip has been observed in the broad peak of the resistance centered at zero bias voltage. That structure has disappeared by increasing the temperature above T_c, which shows its relation to the superconducting character of the electrodes[80]. Although the room-temperature resistances of the samples were comparable to those in the experiment of Ref. [76], no supercurrents have been found in this case. This can be attributed to the large strength of the repulsive electron-electron interaction in the individual nanotubes, supporting the point of view that the superconducting correlations are more likely to develop in ropes of nanotubes.

5.2 Superconductivity inherent to carbon nanotubes

Superconducting properties have been also measured in nanotubes placed between metallic, nonsuperconducting contacts[8, 9]. These experimental observations open the way to use the carbon nanotubes as a testing ground to study superconductivity in molecular wires with a discrete number of conduction channels. It has been already shown that several interesting features arise, as a consequence of the finite number of metallic nanotubes involved and their small length as compared to the size of macroscopic conductors.

One of the main factors in the experiments reported in Ref. [8] is the good quality of the contacts produced for the ropes. This is essential to measure the transport properties intrinsic to the nanotubes since, under conditions of low transparency of the junctions, it is the effect of tunneling and Coulomb blockade what is measured at low temperatures, as described above. In the experiments of Ref. [8], the nanotube ropes have been suspended between Pt/Au bilayers by the same technique already used in the proximity-effect experiments[76]. This has allowed to produce devices with a room-temperature resistance ranging from a few kiloohms down to a few hundred ohms. It has been checked that the bilayers used in the experiment do not become superconducting themselves at low temperatures. The fact that they are not the source of some kind of proximity-induced superconductivity in the nanotubes is supported by the absence of the effect in some of the shortest ropes[8].

The most clear observation of superconducting transition has been made in a rope with about 350 nanotubes and length $L \approx 1$ μm [8]. When measuring the resistance of the sample as a function of the temperature, a drop by two orders of magnitude has been observed below ≈ 0.5 K, as shown in Fig. 10. The resistance does not completely vanish below the transition, but reaches a minimum value $R \approx 74\ \Omega$. As remarked in Ref. [8], this is a consequence of the fact that the resistance of a metallic nanotube has a minimum value, given in terms of the quantum of conductance by $(2G_0)^{-1} \approx 6.5$ kΩ. The value $R \approx 74\ \Omega$ of the residual resistance is consistent then with the approximate number of metallic nanotubes in the rope contributing to the conduction in the superconducting state. The superconducting character of the observed transition is reinforced by the behavior under a magnetic field, which tends to decrease the transition temperature as shown in Fig. 10 [8].

The finite length of the ropes can be also determinant in the development of the superconducting transition. In the experiments of Ref. [8], a rope with a room-temperature resistance of about two orders of magnitude below that of the superconducting rope described above has shown no sign of superconductivity at low temperatures (as it can be seen in Fig. 10). The absence of transition has been attributed to the comparatively small length of the rope ($L \approx 0.3$ μm) [8]. It has been argued that the superconducting coherence length has to be smaller than the rope length for the superconductivity to develop, that condition not being satisfied in the case of the smaller rope. Another sample with a resistance of approximately 1 kΩ and length $L \approx 1.6$ μm has shown a clear sign of transition in the drop of the resistance (although at a comparatively low temperature, below 0.15 K, as observed in Fig. 10 [8]).

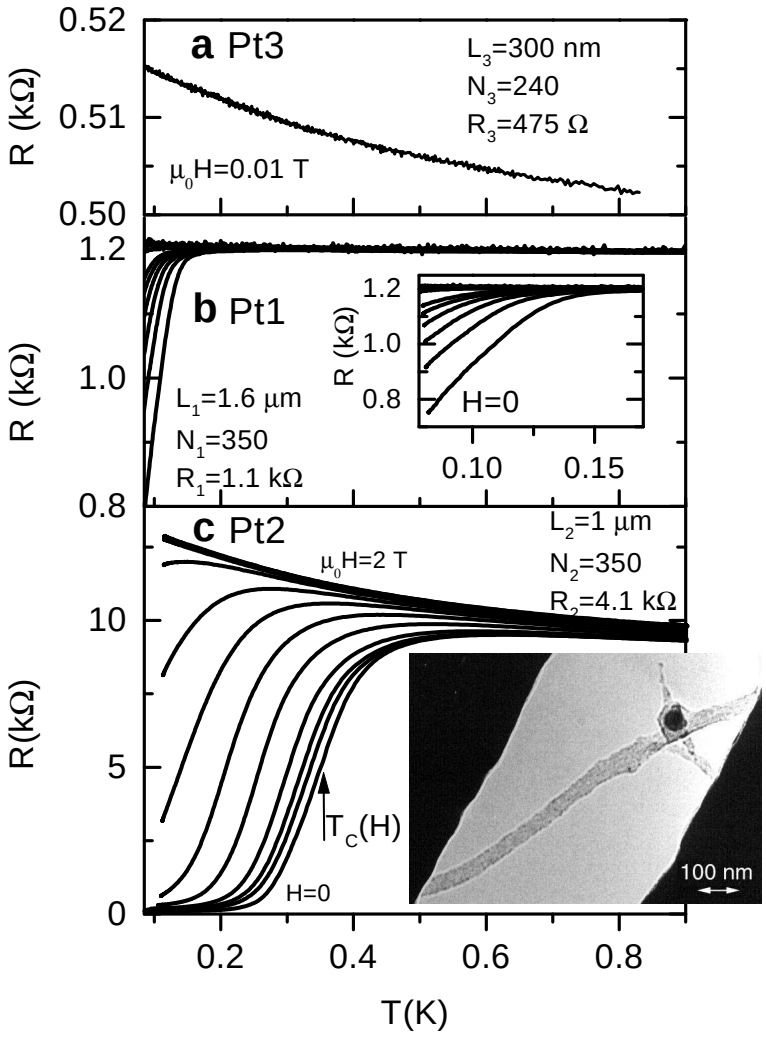

Figure 10: Behavior of the resistance at low temperatures for three different ropes. The length L, the estimated number of nanotubes N and the room-temperature resistance R are indicated in each case. The inset of (b) shows the behavior of sample Pt1 in a magnetic field ranging from 0 up to 1 T. The plot in (c) displays also the dependence of the resistance of sample Pt2 in a magnetic field ranging from 0 up to 2 T (from bottom to top). The inset at the bottom shows a transmission electron microscope image of sample Pt2, with the dark spot corresponding to a Ni/Y catalyst particle. Reprinted from M. Kociak, A. Yu. Kasumov, S. Guéron, B. Reulet, I. I. Khodos, Yu. B. Gorbatov, V. T. Volkov, L. Vaccarini and H. Bouchiat, Phys. Rev. Lett. **86**, 2416 (2001). Copyright 2001 by the American Physical Society.

A consistent explanation of the observed superconducting transitions requires taking into account the mechanism by which the repulsive Coulomb interaction can be overcome in the ropes of nanotubes. The superconducting transition signals the point at which bound electron pairs condensate in the rope. This may happen if there is an effective attractive interaction in the electron liquid[79]. In the first place, it has to be considered that the strength of the Coulomb interaction is strongly reduced in a rope with a large number of metallic nanotubes, for the reasons already presented in the discussion of the proximity-induced superconductivity[81]. Furthermore, a source of attraction between the electrons is needed for the development of the superconductivity intrinsic to the ropes. That attraction arises in the scattering of two electrons by exchange of phonons (i.e. lattice vibrations), in similar manner as it happens in the case of macroscopic superconductors[79].

The effective attraction coming from the coupling of the electrons to the lattice vibrations can naturally overcome the repulsive Coulomb interaction[84, 85]. This is beacuse the former takes place *within* each metallic nanotube of the rope while, as emphasized below Eq. (13), the Coulomb interaction operates in fact in a single interaction channel —that corresponding to the total charge density. Thus, although the strength of the bare Coulomb interaction is larger, the attraction between the electrons through phonon exchange prevails for sufficiently large number of metallic nanotubes in the rope[84, 85]. This argument makes clear that the relevant electron-phonon interactions come from the coupling to *intratube* lattice vibrations. The maximum energies that the optical phonons may reach in the nanotubes, of the order of ~ 0.2 eV [86, 87, 88], are also appropriate to give rise to the superconducting transitions observed experimentally.

Another important factor in the onset of the superconductivity is the small but finite electron tunneling amplitude that exists between the different nanotubes in the rope. These have what has been called *compositional disorder*, meaning that they are made of a mixture of nanotubes with different helicities and diameters[53]. In these circumstances, neighboring nanotubes cannot have their lattices aligned, and this constitutes a great obstacle for conserving the longitudinal momentum when an electron hops from one nanotube to the other. Thus, in a compositionally disordered rope the intertube electron coherence is largely suppressed and the single-particle electron states have to be localized on individual nanotubes[53].

The coupling resistance between tubes in a rope has shown actually wide variations when measured in different experimental samples, with values ranging from 2 MΩ to 140 MΩ [54]. It has been argued that this can be only explained by assuming that transport in the transverse directions of the rope takes place by tunneling between metallic nanotubes of the same helicity. All this is in contrast to the case of an ideal crystalline rope, with perfect alignment of the nanotube lattices, where it has been estimated that the coupling between the nanotubes should give rise to a pseudogap in the density of states of about 0.1 eV [89, 90, 91],

It has been shown however that, when the superconducting correlations develop in the individual nanotubes, the tunneling of Cooper pairs is the mechanism that restablishes the intertube coherence in the rope[84]. The bound electron pairs are formed at zero total momentum, and they are not affected in the tunneling processes

by the misalignement of neighboring nanotube lattices. The intertube coupling established by the tunneling of the electron pairs is a small quantity but, though small it may be, it is essential to account for the superconducting transition in the rope, since in a purely one-dimensional system the electron pairs cannot condensate to form the superconducting state[92]. This becomes possible when there is a coherent propagation along the transverse directions of the rope[84]. The close packing of the bundle of nanotubes (forming a triangular lattice as viewed in a cross-section of the rope) helps in this respect, since each nanotube may have on the average two metallic nearest neighbors, thus making possible the percolation of the Cooper pairs in the transverse directions of the rope.

The coupling of the electrons to the vibrations of the nanotube lattice and the intertube tunneling of the Cooper pairs are the two essential factors in the superconductivity of the ropes. The former can be actually enhanced by dealing with nanotubes of small diameter, since the electron-phonon coupling increases with the curvature of the nanotube[93]. In the experiment reported in Ref. [9], large superconducting correlations have been measured in nanotubes with a diameter of ≈ 4 Å inserted in a zeolite matrix. Such a transversal size is considerably smaller than that of typical nanotubes in a rope, which have a diameter of ≈ 1.4 nm. The measurements of the magnetic susceptibility presented in Ref. [9] show actually the tendency of the zeolite matrix with the nanotubes to expel the magnetic fields below a temperature of ≈ 10 K. This property corresponds to the usual Meissner effect in a macroscopic superconductor. The measurements of the conductance show also an unconventional behavior for a one-dimensional metallic system, in which that observable diverges as the temperature goes to zero[9]. A microscopic description of the large superconducting correlations observed in the nanotubes of short radius must take into account the enhanced electron-phonon coupling[93] as well as their particular band structure, in which more than two subbands cross the Fermi level of the nanotubes[37, 38, 39].

6 Perspectives

Carbon nanotubes have a great potential in the development of electronic devices with diverse functionality since their electronic properties are themselves diverse, depending on the geometry of the nanotube lattice, the contacts used in the devices and the temperature. At room temperature the transport may be ballistic in samples with high structural perfection. In the cases where the contacts create tunnel junctions, one can expect nonlinear I–V characteristics which are the signature of the Luttinger liquid behavior. At much lower temperatures, quantum interference effects in the propagation of the electrons can be observed in samples with highly transparent contacts while, in the case of very thick ropes, the reduction in the strength of the Coulomb interaction may give rise to the superconductivity of the nanotubes.

The first step towards the use of the carbon nanotubes in molecular electronics requires the integration of several nanotube devices in order to produce the desired

functionality. Important progress is already being made in this direction. In Ref. [15], the architecture of two perpendicularly crossed arrays of nanotubes has been proposed as a model for a nonvolatile random access memory. Each crossing point for two perpendicular nanotubes constitutes an addressable device element. The junctions have two stable positions, with a different separation between the crossed nanotubes that can be controlled electromechanically. This allows the definition of ON and OFF states at each crossing point, characterized by respective resistances which may differ in general by orders of magnitude. The feasibility of the proposal has been supported by the realization and investigation of junctions made of crossed ropes of nanotubes[15]. The measurement of the I–V characteristics of crossed nanotube junctions has been also accomplished in Ref. [94], with different combinations of individual single-walled nanotubes with metallic and semiconducting character.

Another experimental accomplishment which has opened the way for a nanotube-based electronics can be found in Ref. [16]. It has been reported there the construction of the first circuit based on a single nanotube capable of performing a logic operation. The circuit represents what is called a voltage inverter, by which a logical 1 can be transformed into a logical 0 and viceversa. This is the realization of the NOT logic function, that is combined with the AND and OR logic operations to build the complex structure of modern microprocessors. A new experimental development has been needed in the construction of the logic circuit, since this requires to place in series two field-effect transistors being respectively of n-type (with excess of conduction electrons) and p-type (with conduction achieved by electron holes). While nanotubes are usually found with the latter character, the transformation to n-type has to be accomplished by doping the nanotubes with alkali metals or, in a simpler way, by heating the nanotubes in a vacuum as shown in Ref. [95]. An important feature of the circuit is the gain, that relates the strength of the output to that of the input signal and which, in this case, reaches the value of 1.6 . This opens the possibility of assembling gates of the kind proposed into more complex circuits.

The operation of several small circuits built from the combination of nanotube field-effect transistors has been also shown in Ref. [17]. What is special in the integration of these devices is that each nanotube transistor has its own local gate, so that the effect of doping by varying the corresponding gate voltage can be controlled independently in each nanotube. A very large capacitive coupling has been achieved between the semiconducting nanotube and the nearby gate, making thus possible to shift the Fermi level in the nanotube from the valence band (p-doped regime) to the conduction band (n-doped regime) under variations in the gate voltage. In this way, the integration of the nanotube transistors has allowed to realize several logic circuits, like an inverter, a NOR logic element or a static random access memory element.

An interesting finding has been that the field-effect transistors made of single nanotubes can have better performance that the leading silicon transistor prototypes[96]. This has been realized in the process of building nanotube-based transistors with larger capacitive coupling between the nanotube and the gate electrode, that controls the density of charge carriers in the molecule. The advances in the design of

the transistors have come from placing the gate electrode on top of the nanotube and using a thinner dielectric between them[96]. Thus, smaller variations in the voltage of the gate electrode can lead to significant changes in the resistance of the nanotube. This new kind of transistors has led to a high transconductance (the measure of the capability to carry electric current) at low voltages, outperforming in this respect the best silicon transistor prototypes[96].

The route towards the large-scale integration of nanotube devices presents great complexities, but carbon nanotubes have already shown the potential for more straightforward applications. One of them arises from the strong coupling between the electronic properties and mechanical deformations, that may include the twist[97], bending[98] or stretching[99, 100, 101, 102] of the carbon nanotubes. It has been shown that, in the case of semiconducting nanotubes, a semiconductor-metal transition can take place upon application of sufficient uniaxial strain[102]. The reverse trend has been also measured, by pushing a metallic carbon nanotube with the tip of an atomic force microscope to produce a decrease of nearly two orders of magnitude in the conductance[103, 104, 105]. These observations open the way to use carbon nanotubes as nanoscale mechanical sensors.

The carbon nanotubes have also shown the potential for piezoelectric applications. The injection of charge into the nanotubes can alter their structure, due to the fact that the carbon-carbon bonds modify their lengths according to the electrons or holes added[106]. These effects have been investigated in nanotube sheets, which are made of highly entangled mats of nanotube bundles. In the experiments reported in Ref. [107], the changes in the length of strips of such kind of nanotube paper have been measured as a function of the applied voltage, carrying the operation within a NaCl electrolyte. Thus, the expansion or contraction of the strips has been the result of the injection of electronic charge from the electrodes to the surface of the nanotube bundles, with the electrolyte ions forming layers of respective opposite charges to balance those in the nanotubes[107]. The electromechanical actuators thus designed have shown good performance, being able to generate higher stresses than those of natural muscles. An important advantage over conventional ferroelectric actuators is that the nanotube sheets can provide large strains with applied voltages of just a few volts. The mechanical performance should be enhanced in the case of nonbundled nanotubes, and it has been estimated that, for the sheets made of separate nanotubes, the actuator strain could be of the order of ~ 1 %[107]. A number of possible uses of the nanotube actuators have been proposed, from biomedical applications to flow control at high temperatures.

It has been also suggested the application of carbon nanotubes as chemical sensors. The nanotubes have the tendency to adsorb gas molecules in their surface. In the case of semiconducting nanotubes, this has been shown to lead to significant changes in the conduction properties[108, 109]. The gas molecules give rise to a transfer of charge that makes the nanotubes to become p-doped semiconductors. The change in their conductivity can give then a measure of very small concentrations of particles in the chemical environment at room temperature, in a much more sensitive way than existing chemical sensors.

Carbon nanotubes can be used as tips in scanning probe microscopes, what

provides several advantages over usual silicon tips[110, 111]. The ability that the nanotube tips have to buckle elastically reduces the damage that can be produced when crashing into the sample. They lead to an improvement of the resolution, as a consequence of their small diameter. Moreover, they can be modified at the ends to enable the manipulation of structures at the molecular scale[112]. The construction of nanoscale tweezers has been also possible by attaching a pair of carbon nanotubes to respective electrodes, and controlling the nanotube arms by the voltage applied between them[113]. Such a device has made possible the manipulation of different structures at the nanometer scale.

Finally, the technological applications of carbon nanotubes can also have a more direct impact in every-day life. They have been proposed for the construction of supercapacitors, which may take advantage of the large surface area accessible in nanotube arrays. These can give rise to capacitors with high power and storage capabilities. Anyhow, the carbon nanotubes may find the most interesting commercial application as electron sources in field-emission devices[114, 115]. These can be used in flat panel displays, as well as in lamps and x-ray sources. The emission is produced by applying a voltage between a surface with nanotube fibers, acting as a cathode, and a substrate with phosphor arrays. The high local fields created in the nanotube geometry make the electrons to jump towards the anode, where the contact with the phosphor produces the spots of light in the display. The flat panel nanotube displays turn out to save more energy and to have higher brightness than liquid crystal displays. A similar field-emission effect can be applied to the generation of x-rays, when the anode is replaced by a metal surface, what can lead to interesting applications for medical purposes. All these developments stress once more the significance that the phenomena taking place in minute devices can have for the construction of useful engines, tailored for the needs of our time.

Aknowledgements.— It is a pleasure to thank M. Bockrath, H. Bouchiat, C. Dekker, C. M. Lieber and C. Schönenberger, for the help granted with the graphic material of this contribution.

7 Appendix: Physical constants of carbon nanotubes

Physical property	
Minimum intrinsic resistance (individual metallic single-walled nanotubes)	≈ 6.5 kΩ
Bandgap (semiconducting nanotubes)	~ 0.5 eV [35, 36]
Energy gap ("metallic" zig-zag nanotubes)	~ 0.05 eV [43]
Dielectric constant (single-walled nanotubes on Si/SiO_2 substrate)	≈ 1.4 [5, 55]
Charging energy (~ 3 μm long single-walled nanotube)	~ 2.5 meV [5]
Charging energy (~ 2 μm long multi-walled nanotube)	~ 0.5 meV [68]
Intertube resistance (nanotube ropes)	$\gtrsim 1$ MΩ [54]
Superconducting transition temperature (nanotube ropes)	~ 0.5 K [8]
Critical supercurrent (nanotube rope between Au/Re contacts)	~ 1 μA [76]
Current density (multi-walled nanotubes)	$> 10^9$ A/cm^2 [116]
Mobility (semiconducting nanotubes at room temperature)	$> 20,000$ cm^2/Vs [117]

References

[1] S. Iijima, Nature **354**, 56 (1991).

[2] R. Saito, G. Dresselhaus and M. S. Dresselhaus, *Physical Properties of Carbon Nanotubes*, Imperial College Press, London (1998).

[3] M. S. Dresselhaus, G. Dresselhaus and P. C. Eklund, *Science of Fullerenes and Carbon Nanotubes*, Academic Press, New York (1996).

[4] M. Bockrath, D. H. Cobden, P. L. McEuen, N. G. Chopra, A. Zettl, A. Thess and R. E. Smalley, Science **275**, 1922 (1997).

[5] S. J. Tans, M. H. Devoret, H. Dai, A. Thess, R. E. Smalley, L. J. Geerligs and C. Dekker, Nature **386**, 474 (1997).

[6] W. Liang, M. Bockrath, D. Bozovic, J. H. Hafner, M. Tinkham and H. Park, Nature **411**, 665 (2001).

[7] S. Frank, P. Poncharal, Z. L. Wang and W. A. de Heer, Science **280**, 1744 (1998).

[8] M. Kociak, A. Yu. Kasumov, S. Guéron, B. Reulet, I. I. Khodos, Yu. B. Gorbatov, V. T. Volkov, L. Vaccarini and H. Bouchiat, Phys. Rev. Lett. **86**, 2416 (2001).

[9] Z. K. Tang, L. Zhang, N. Wang, X. X. Zhang, G. H. Wen, G. D. Li, J. N. Wang, C. T. Chan and P. Sheng, Science **292**, 2462 (2001).

[10] Z. Yao, H. W. Ch. Postma, L. Balents and C. Dekker, Nature **402**, 273 (1999).

[11] S. J. Tans, A. R. M. Verschueren and C. Dekker, Nature **393**, 49 (1998).

[12] R. Martel, T. Schmidt, H. R. Shea, T. Hertel and Ph. Avouris, Appl. Phys. Lett. **73**, 2447 (1998).

[13] C. Zhou, J. Kong and H. Dai, Appl. Phys. Lett. **76**, 1597 (1999).

[14] H. W. Ch. Postma, T. Teepen, Z. Yao, M. Grifoni and C. Dekker, Science **293**, 76 (2001).

[15] T. Rueckes, K. Kim, E. Joselevich, G. Y. Tseng, C.-L. Cheung and C. M. Lieber, Science **289**, 94 (2000).

[16] V. Derycke, R. Martel, J. Appenzeller and Ph. Avouris, Nano Letters **1**, 453 (2001).

[17] A. Bachtold, P. Hadley, T. Nakanishi and C. Dekker, Science **294**, 1317 (2001).

[18] N. Hamada, S. Sawada and A. Oshiyama, Phys. Rev. Lett. **68**, 1579 (1992).

[19] R. Saito, M. Fujita, G. Dresselhaus and M. S. Dresselhaus, Appl. Phys. Lett. **60**, 2204 (1992).

[20] J. W. Mintmire, B. I. Dunlap and C. T. White, Phys. Rev. Lett. **68**, 631 (1992).

[21] L. Chico, V. H. Crespi, L. X. Benedict, S. G. Louie and M. L. Cohen, Phys. Rev. Lett. **76**, 971 (1996).

[22] R. Saito, G. Dresselhaus and M. S. Dresselhaus, Phys. Rev. B **53**, 2044 (1996).

[23] Ph. Lambin, A. Fonseca, J. P. Vigneron, J. B. Nagy and A. A. Lucas, Chem. Phys. Lett. **245**, 85 (1995).

[24] M. Menon and D. Srivastava, Phys. Rev. Lett. **79**, 4453 (1997).

[25] M. Menon and D. Srivastava, J. Mat. Res. **13**, 2357 (1998).

[26] C. Papadopoulos, A. Rakitin, J. Li, A. S. Vedeneev, J. M. Xu, Phys. Rev. Lett. **85**, 3476 (2000).

[27] B. C. Satishkumar, P. J. Thomas, A. Govindaraj and C. N. R. Rao, Appl. Phys. Lett. **77**, 2530 (2000).

[28] A. N. Andriotis, M. Menon, D. Srivastava and L. Chernozatonskii, Phys. Rev. Lett. **87**, 066802 (2001).

[29] A. N. Andriotis, M. Menon, D. Srivastava and L. Chernozatonskii, Appl. Phys. Lett. **79**, 266 (2001).

[30] B. W. Smith, M. Monthioux and D. E. Luzzi, Nature **396**, 323 (1998).

[31] K. Hirahara, K. Suenaga, S. Bandow, H. Kato, T. Okazaki, H. Shinohara and S. Iijima, Phys. Rev. Lett. **85**, 5384 (2000).

[32] S. Okada, S. Saito and A. Oshiyama, Phys. Rev. Lett. **86**, 3835 (2001).

[33] J. Lee, H. Kim, S.-J. Kahng, G. Kim, Y.-W. Son, J. Ihm, H. Kato, Z. W. Wang, T. Okazaki, H. Shinohara and Y. Kuk, Nature **415**, 1005 (2002).

[34] D. J. Hornbaker, S.-J. Kahng, S. Misra, B. W. Smith, A. T. Johnson, E. J. Mele, D. E. Luzzi and A. Yazdani, Science **295**, 828 (2002).

[35] J. W. G. Wildöer, L. C. Venema, A. G. Rinzler, R. E. Smalley and C. Dekker, Nature **391**, 59 (1998).

[36] T. W. Odom, J.-L. Huang, P. Kim and C. M. Lieber, Nature **391**, 62 (1998).

[37] X. Blase, L. X. Benedict, E. L. Shirley and S. G. Louie, Phys. Rev. Lett. **72**, 1878 (1994).

[38] O. Gülseren, T. Yildirim and S. Ciraci, Phys. Rev. B **65**, 153405 (2002).

[39] K. Kanamitsu, J. Phys. Soc. Japan **71**, 483 (2002).

[40] J. González, F. Guinea and M. A. H. Vozmediano, Nucl. Phys. **B406**, 771 (1993).

[41] J. A. Stroscio and R. M. Feenstra, in *Scanning Tunneling Microscopy* edited J. A. Stroscio and W. J. Kaiser, Academic, New York (1993), p. 95-141.

[42] J. W. Mintmire, D. H. Robertson and C. T. White, J. Phys. Chem. Solids **54**, 1835 (1993).

[43] M. Ouyang, J.-L. Huang, C.-L. Cheung and C. M. Lieber, Science **292**, 702 (2001).

[44] C. T. White, D. H. Robertson and J. W. Mintmire, in *Clusters and Nanostructured Materials*, edited P. Jena and S. Behera, Nova, New York (1996), p. 231.

[45] M. Ouyang, J.-L. Huang, C.-L. Cheung and C. M. Lieber, Science **291**, 97 (2001).

[46] V. J. Emery, in *Highly Conducting One-Dimensional Solids*, edited J. T. Devreese, R. P. Evrard and V. E. Van Doren, Plenum, New York (1979).

[47] J. Sólyom, Adv. Phys. **28**, 201 (1979).

[48] L. Chico, L. X. Benedict, S. G. Louie and M. L. Cohen, Phys. Rev. B **54**, 2600 (1996).

[49] H. Grabert and M. H. Devoret, *Single Charge Tunneling*, Plenum, New York (1992).

[50] M. Bockrath, D. H. Cobden, J. Lu, A. G. Rinzler, R. E. Smalley, L. Balents and P. L. McEuen, Nature **397**, 598 (1999).

[51] M. P. A. Fisher and A. Dorsey, Phys. Rev. Lett. **54**, 1609 (1985).

[52] H. Grabert and U. Weiss, Phys. Rev. Lett. **54**, 1605 (1985).

[53] A. A. Maarouf, C. L. Kane and E. J. Mele, Phys. Rev. B **61**, 11156 (2000).

[54] H. Stahl, J. Appenzeller, R. Martel, Ph. Avouris and B. Lengeler, Phys. Rev. Lett. **85**, 5186 (2000).

[55] R. Egger and A. O. Gogolin, Phys. Rev. Lett. **79**, 5082 (1997).

[56] C. Kane, L. Balents and M. P. A. Fisher, Phys. Rev. Lett. **79**, 5086 (1997).

[57] R. Landauer, J. Phys. Cond. Matter **1**, 8099 (1989).

[58] R. Landauer, Philos. Mag. **21**, 863 (1970).

[59] S. Datta, *Electronic Transport Properties in Mesoscopic Systems*, Cambridge Univ. Press, Cambridge (1995).

[60] S. Sanvito, Y.-K. Kwon, D. Tománek and C. J. Lambert, Phys. Rev. Lett. **84**, 1974 (2000).

[61] P. J. de Pablo, C. Gómez-Navarro, J. Colchero, P. A. Serena, J. Gómez-Herrero and A. M. Baró, Phys. Rev. Lett. **88**, 036804 (2002).

[62] L. C. Venema, J. W. G. Wildöer, J. W. Janssen, S. J. Tans, H. L. J. Temminck Tuinstra, L. P. Kouwenhoven and C. Dekker, Science **283**, 52 (1999).

[63] A. Bachtold, C. Strunk, J.-P. Salvetat, J.-M. Bonard, L. Forró, T. Nussbaumer and C. Schönenberger, Nature **397**, 673 (1999).

[64] C. L. Kane and M. P. A. Fisher, Phys. Rev. Lett. **68**, 1220 (1992).

[65] C. L. Kane and M. P. A. Fisher, Phys. Rev. B **46**, 15233 (1992).

[66] C. T. White and T. N. Todorov, Nature **393**, 240 (1998).

[67] C. W. J. Beenakker, Phys. Rev. B **44**, 1646 (1991).

[68] M. R. Buitelaar, A. Bachtold, T. Nussbaumer, M. Iqbal and C. Schönenberger, Phys. Rev. Lett. **88**, 156801 (2002).

[69] M. Krüger, M. R. Buitelaar, T. Nussbaumer and C. Schönenberger, Appl. Phys. Lett. **78**, 1291 (2001).

[70] S. Tarucha, D. G. Austing, Y. Tokura, W. G. van der Wiel and L. P. Kouwenhoven, Phys. Rev. Lett. **84**, 2485 (2000).

[71] J. Nygård, D. H. Cobden and P. E. Lindelof, Nature **408**, 342 (2000).

[72] L. P. Kouwenhoven and L. Glazman, Phys. World **14**, 33 (2001).

[73] L. Chico, M. P. López Sancho and M. C. Muñoz, Phys. Rev. Lett. **81**, 1278 (1998).

[74] M. Bockrath, W. Liang, D. Bozovic, J. H. Hafner, C. M. Lieber, M. Tinkham and H. Park, Science **291**, 283 (2001).

[75] M. T. Woodside and P. L. McEuen, Science **296**, 1098 (2002).

[76] A. Yu. Kasumov, R. Deblock, M. Kociak, B. Reulet, H. Bouchiat, I. I. Khodos, Yu. B. Gorbatov, V. T. Volkov, C. Journet and M. Burghard, Science **284**, 1508 (1999).

[77] D. Esteve, H. Pothier, S. Guéron, N. O. Birge, M. H. Devoret, in *Mesoscopic Electron Transport*, edited L. L. Sohn, L. P. Kouwenhoven and G. Schön, Kluwer, Dordrecht (1997), p. 375.

[78] B. J. van Wees and H. Takayanagi, in *Mesoscopic Electron Transport*, edited L. L. Sohn, L. P. Kouwenhoven and G. Schön, Kluwer, Dordrecht (1997), p. 469.

[79] M. Tinkham, *Introduction to Superconductivity*, McGraw-Hill, Singapore (1996).

[80] A. F. Morpurgo, J. Kong, C. M. Marcus and H. Dai, Science **286**, 263 (1999).

[81] J. González, Phys. Rev. Lett. **87**, 136401 (2001).

[82] D. L. Maslov, M. Stone, P. M. Goldbart and D. Loss, Phys. Rev. B **53**, 1548 (1996).

[83] R. Fazio, F. W. J. Hekking and A. A. Odintsov, Phys. Rev. B **53**, 6653 (1996).

[84] J. González, Phys. Rev. Lett. **88**, 076403 (2002).

[85] J. González, Phys. Rev. B (in press).

[86] D. Sánchez-Portal, E. Artacho, J. M. Soler, A. Rubio and P. Ordejón, Phys. Rev. B **59**, 12678 (1999).

[87] L. M. Woods and G. D. Mahan, Phys. Rev. B **61**, 10651 (2000).

[88] R. Saito, A. Jorio, A. G. Souza Filho, G. Dresselhaus, M. S. Dresselhaus and M. A. Pimenta, Phys. Rev. Lett. **88**, 027401 (2002).

[89] P. Delaney, H. Joon Choi, J. Ihm, S. G. Louie and M. L. Cohen, Nature **391**, 466 (1998).

[90] Y.-K. Kwon, S. Saito and D. Tománek, Phys. Rev. B **58**, R13314 (1998).

[91] J.-C. Charlier, X. Gonze and J.-P. Michenaud, Europhys. Lett. **29**, 43 (1995).

[92] H. J. Schulz, in *Correlated Electron Systems*, edited V. J. Emery, World Scientific, Singapore (1993), Vol. 9.

[93] L. X. Benedict, V. H. Crespi, S. G. Louie and M. L. Cohen, Phys. Rev. B **52**, 14935 (1995).

[94] M. S. Fuhrer, J. Nygård, L. Shih, M. Forero, Y.-G. Yoon, M. S. C. Mazzoni, H. J. Choi, J. Ihm, S. G. Louie, A. Zettl and P. L. McEuen, Science **288**, 494 (2000).

[95] V. Derycke, R. Martel, J. Appenzeller and Ph. Avouris, Appl. Phys. Lett. **80**, 2773 (2002).

[96] S. J. Wind, J. Appenzeller, R. Martel, V. Derycke and Ph. Avouris, Appl. Phys. Lett. **80**, 3817 (2002).

[97] C. L. Kane and E. J. Mele, Phys. Rev. Lett. **78**, 1932 (1997).

[98] A. Rochefort, D. R. Salahub and Ph. Avouris, Chem. Phys. Lett. **297**, 45 (1998).

[99] R. Heyd, A. Charlier and E. McRae, Phys. Rev. B **55**, 6820 (1997).

[100] V. H. Crespi, M. L. Cohen and A. Rubio, Phys. Rev. Lett. **79**, 2093 (1997).

[101] P. Zhang, P. E. Lammert and V. H. Crespi, Phys. Rev. Lett. **81**, 5346 (1998).

[102] L. Yang and J. Han, Phys. Rev. Lett. **85**, 154 (2000).

[103] T. W. Tombler, C. Zhou, L. Alexseyev, J. Kong, H. Dai, L. Liu, C. S. Jayanthi, M. Tang and S.-Y. Wu, Nature **405**, 769 (2000).

[104] L. Liu, C. S. Jayanthi, M. Tang, S.-Y. Wu, T. W. Tombler, C. Zhou and L. Alexseyev, Phys. Rev. Lett. **84**, 4950 (2000).

[105] A. Maiti, A. Svizhenko and M. P. Anantram, Phys. Rev. Lett. **88**, 126805 (2002).

[106] Yu. N. Gartstein, A. A. Zakhidov and R. H. Baughman, Phys. Rev. Lett. **89**, 045503 (2002).

[107] R. H. Baughman, C. Cui, A. A. Zakhidov, Z. Iqbal, J. N. Barisci, G. M. Spinks, G. G. Wallace, A. Mazzoldi, D. De Rossi, A. G. Rinzler, O. Jaschinski, S. Roth and M. Kertesz, Science **284**, 1340 (1999).

[108] J. Kong, N. R. Franklin, C. Zhou, M. G. Chapline, S. Peng, K. Cho and H. Dai, Science **287**, 622 (2000).

[109] P. G. Collins, K. Bradley, M. Ishigami and A. Zettl, Science **287**, 1801 (2000).

[110] H. Dai, J. H. Hafner, A. G. Rinzler, D. T. Colbert and R. E. Smalley, Nature **384**, 147 (1996).

[111] J. H. Hafner, C. L. Cheung and C. M. Lieber, Nature **398**, 761 (1999).

[112] S. S. Wong, E. Joselevich, A. T. Woolley, C. L. Cheung and C. M. Lieber, Nature **394**, 52 (1998).

[113] P. Kim and C. M. Lieber, Science **286**, 2148 (1999).

[114] A. G. Rinzler, J. H. Hafner, P. Nikolaev, L. Lou, S. G. Kim, D. Tománek, P. Nordlander, D. T. Colbert and R. E. Smalley, Science **269**, 1550 (1995).

[115] W. A. de Heer, A. Châtelain and D. Ugarte, Science **270**, 1179 (1995).

[116] P. G. Collins, M. Hersam, M. Arnold, R. Martel and Ph. Avouris, Phys. Rev. Lett. **86**, 3128 (2001).

[117] T. Dürkop, T. Brintlinger and M. S. Fuhrer, in *Structural and Electronic Properties of Molecular Nanostructures*, edited H. Kuzmany, J. Fink, M. Mehring and S. Roth, AIP Conference Proceedings, New York (2002), p. 242-246.